

GRAVITATIONAL LENSING

LECTURE 23

Docente: Massimo Meneghetti
AA 2016-2017

STRONG LENSING BY GALAXIES AND CLUSTERS

- Rethinking galaxies and galaxy clusters as strong lenses
- Finding strong lenses
- Applications:
 - the mass structure of galaxies and clusters
 - substructures
 - cosmography
 - cosmic telescopes



lens oriented



source oriented

LENSING OBSERVABLES

- multiple images [images with the same colors and the same spectra]
- parity inversion in multiple images
- image distortions
- time delays

HOW TO FIND STRONG LENSES

- Requirements:
 - good spatial resolution (<0.2'')
 - survey area/speed/depth (many objects at once or fast one-by-one)
 - contrast between sources and lenses
 - time sampling
- Until recently, these conditions have been difficult to meet...
- Search potential lenses or potential sources, employing
 - optical/radio imaging
 - spectroscopy
 - variability
- and follow-up...

SERENDIPITOUS DISCOVERIES

Discovery of the first galaxy-QSO lens system (1979)

0957+561 A, B: twin quasistellar objects or gravitational lens?

D. Walsh

University of Manchester, Nuffield Radio Astronomy Laboratories, Jodrell Bank, Macclesfield, Cheshire, UK

R. F. Carswell

Institute of Astronomy, Cambridge, UK

R. J. Weymann

Steward Observatory, University of Arizona, Tucson, Arizona 85721

0957+561 A, B are two QSOs of mag 17 with 5.7 arc s separation at redshift 1.405. Their spectra leave little doubt that they are associated. Difficulties arise in describing them as two distinct objects and the possibility that they are two images of the same object formed by a gravitational lens is discussed.

SPECTROSCOPIC observations have been in progress for several years on QSO candidates using a survey of radio sources made at 966 MHz with the MkIA telescope at Jodrell Bank. Many of the identifications have been published by Cohen *et al.*¹ with interferometric positions accurate to ~2 arc s and a further list has been prepared by Porcas *et al.*². The latter list consists of sources that were either too extended or too confused for accurate interferometric positions to be measured, and these were observed with the pencil-beam of the 300 ft telescope at NRAO, Green Bank at λ 6 cm and λ 11 cm. This gave positions with typical accuracy 5–10 arc s and the identifications are estimated as ~80% reliable.

The list of Porcas *et al.* includes the source 0957+561 which has within its field a close pair of blue stellar objects, separated by ~6 arc s, which are suggested as candidate identifications. Their positions and red and blue magnitudes, m_R and m_B , estimated from the Palomar Observatory Sky Survey (POSS) are given in Table 1 and a finding chart is given in Fig. 1. Since the images on the POSS overlap, the magnitude estimates may

be of lower accuracy than normal, but they are very nearly equal and object A is definitely bluer than object B. The mean position of the two objects is 17 arc s from the radio position, so the identification is necessarily tentative.

Observations

The two objects 0957+561 A, B were observed on 29 March 1979 at the 2.1 m telescope of the Kitt Peak National Observatory (KPNO) using the intensified image dissector scanner (IIDS). Sky subtraction was used with circular apertures separated by 99.4 arc s. Some observational parameters are given in Table 2. The spectral range was divided into 1,024 data bins, each bin 3.5 Å wide, and the spectral resolution was 16 Å. After 20-min integration on each object it was clear that both were QSOs with almost identical spectra and redshifts of ~1.40 on the basis of strong emission lines identified as C IV λ 1549 and C III] λ 1909. Further observations were made on 29 March and on subsequent nights as detailed in Table 2. By offsetting to observe empty sky a few arc seconds from one object on both 29 and 30 March it was confirmed that any contamination of the spectrum of one object by light from the other was negligible.

Table 1 Positions and magnitudes of 0957+561 A, B

Object	RA	Dec (1950.0)	M_R	M_B
0957+561A	09 57 57.3	+56 08 22.9	17.0	16.7
0957+561B	09 57 57.4	+56 08 16.9	17.0	17.0

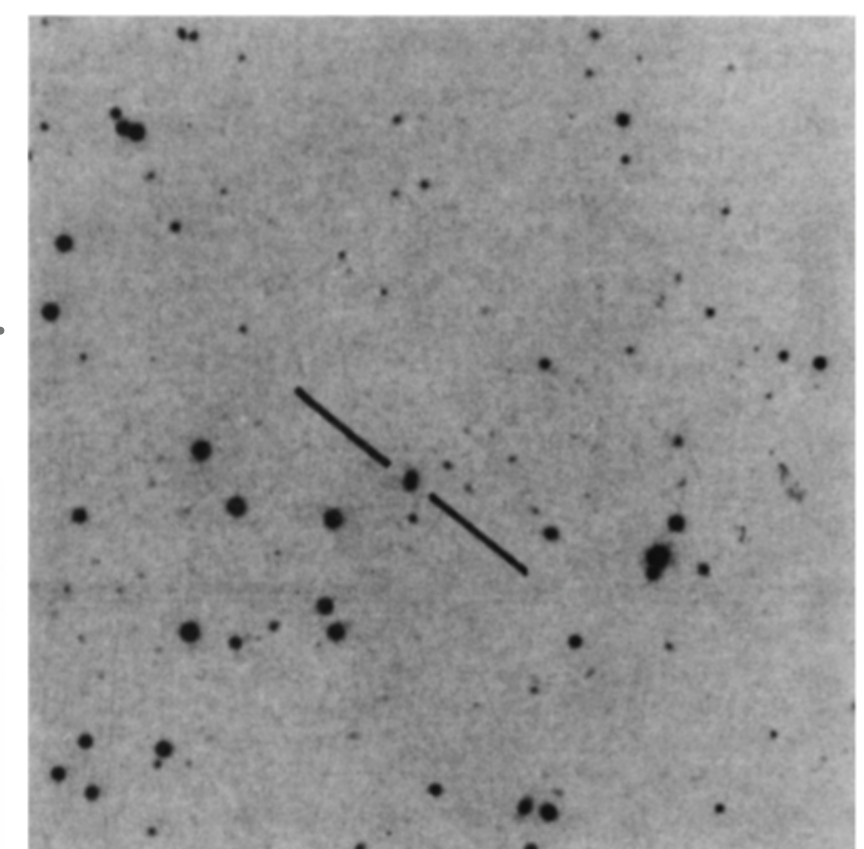


Fig. 1 Finding chart for the QSOs 0957+561 A and B. The chart is 8.5 arc min square with the top right hand corner north preceding and is from the E print of the POSS.

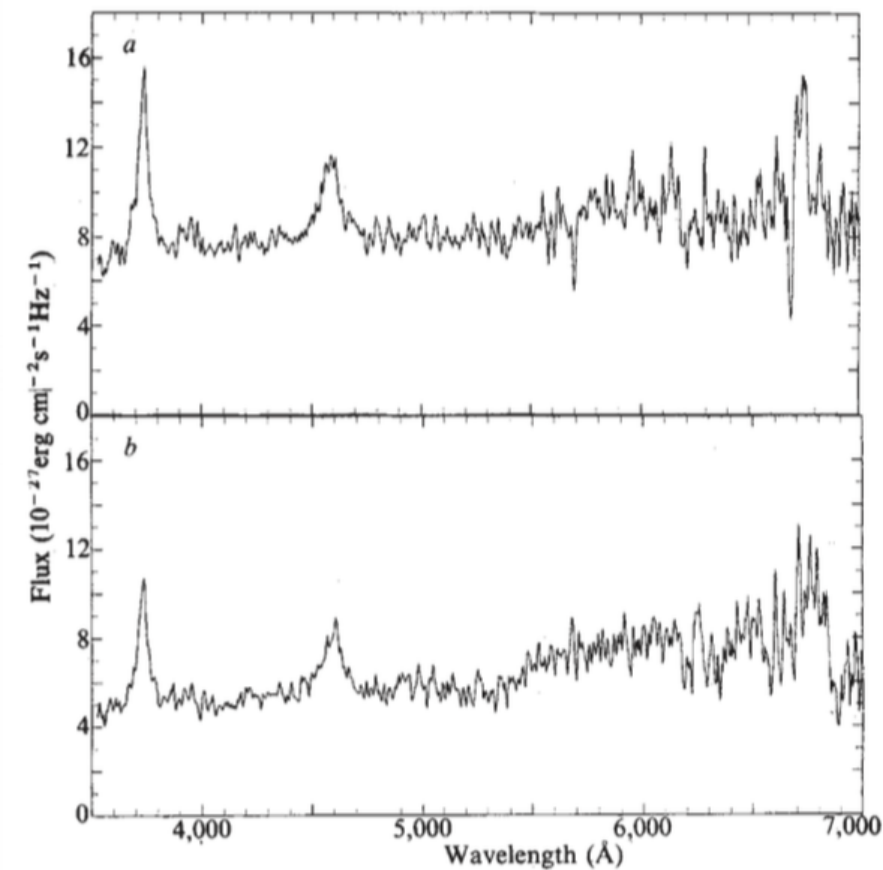


Fig. 2 IIDS scans of 0957+561 A(a) and B(b). The data are smoothed over 10 Å and the spectral resolution is 16 Å.

SE

Disc

095
obje

D. Wal

University o

R. F. C

Institute of

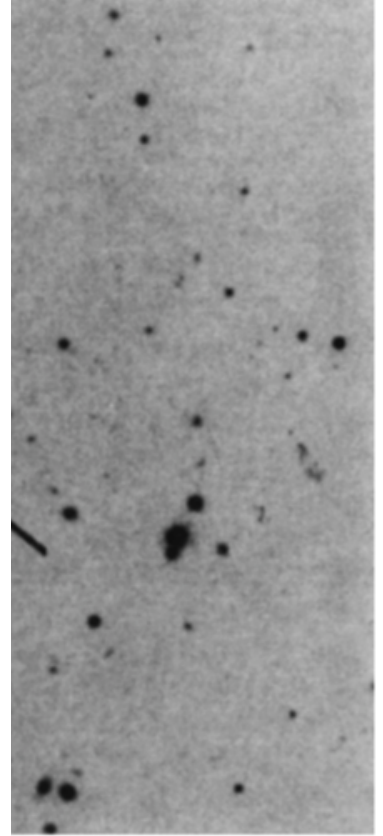
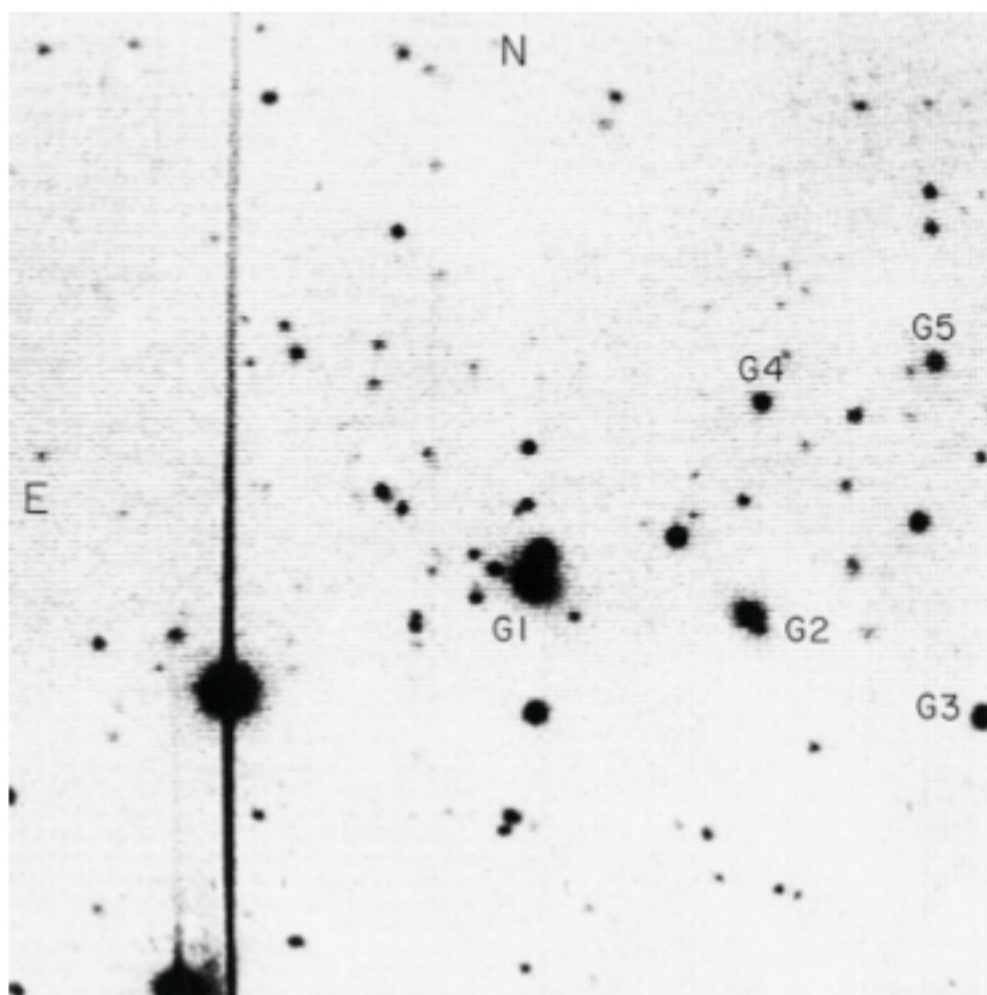
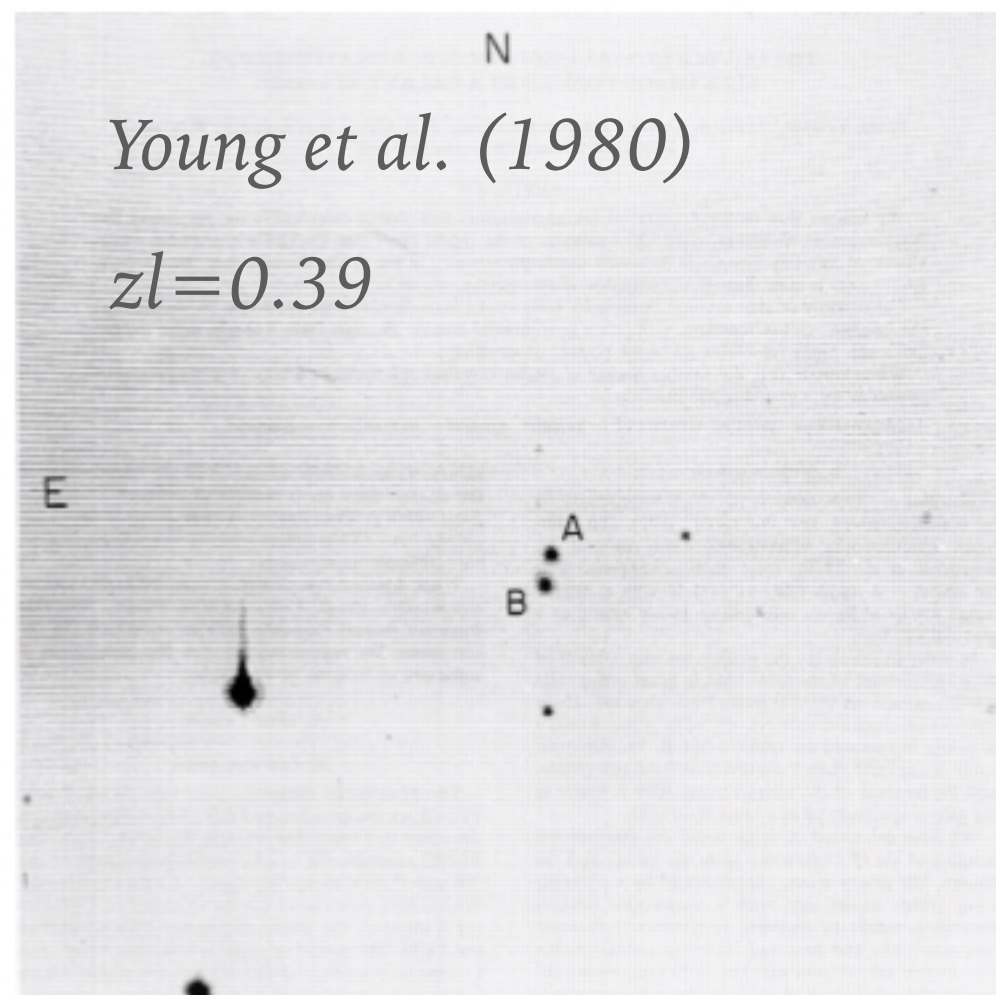
R. J. V

Steward Ob

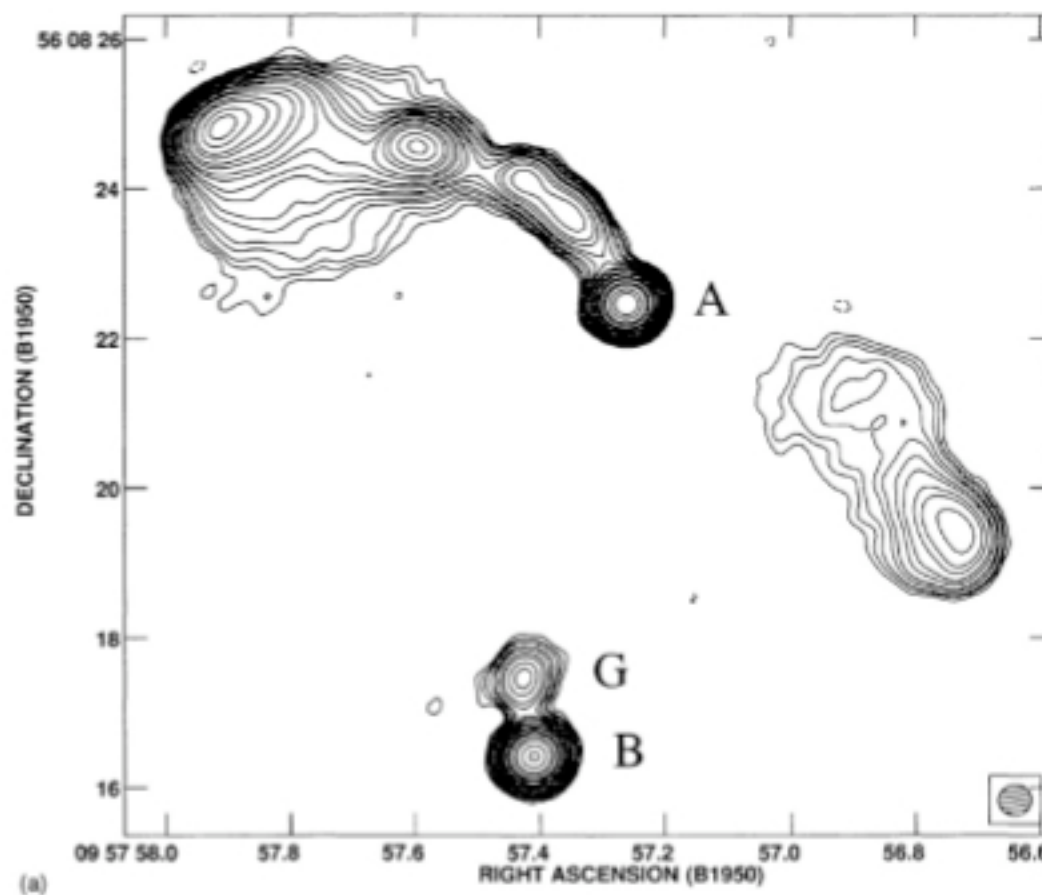
0957 + 56
separation
that they
them as two
two image
lens is dis

SPECTROS
several yea
made at 96
Many of the
with interf
list has bee
sources tha
accurate in
were obser
NRAO, Gr
with typica
estimated a

The list c
has within i
by ~6 arc s
Their posit
estimated f
are given in
the images



957 + 561 A and B. The chart at hand corner north preceding it of the POSS.



Gorenstein et al. (1984)

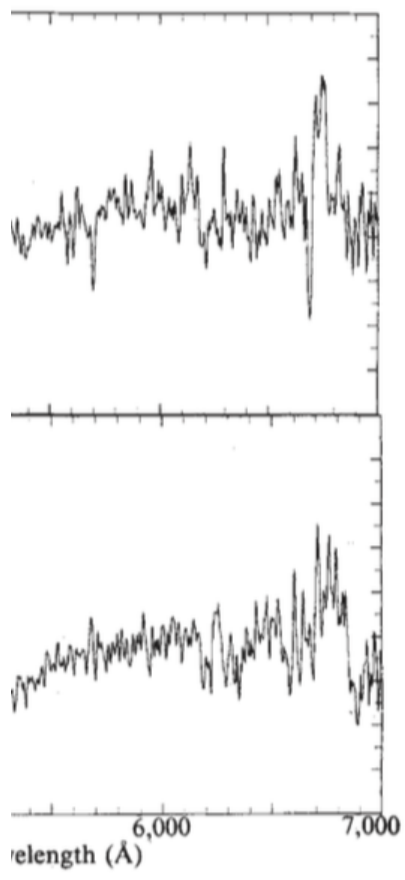
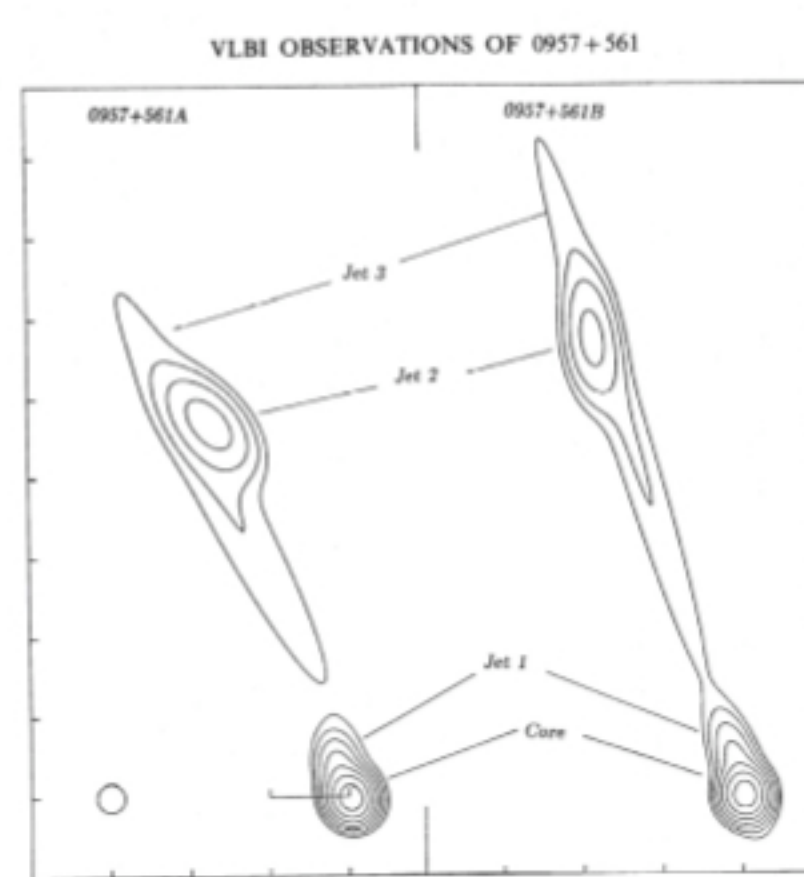
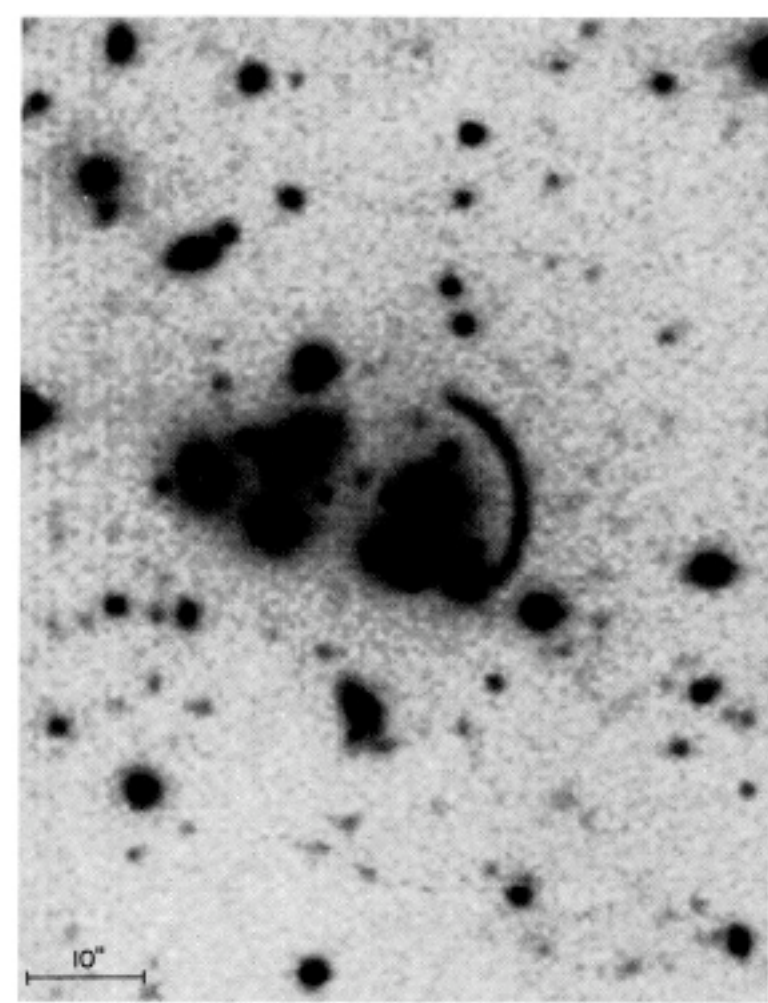
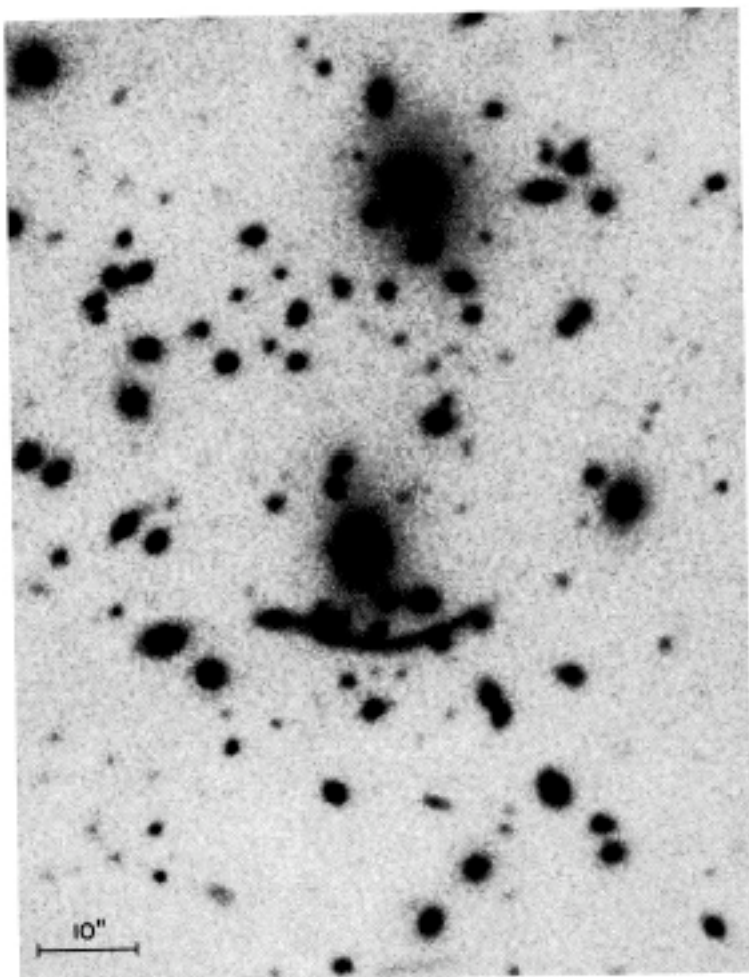


Fig. 2 HJD scans of 0957 + 561 A(a) and B(b). The data are smoothed over 10 Å and the spectral resolution is 16 Å.

SERENDIPITOUS DISCOVERIES

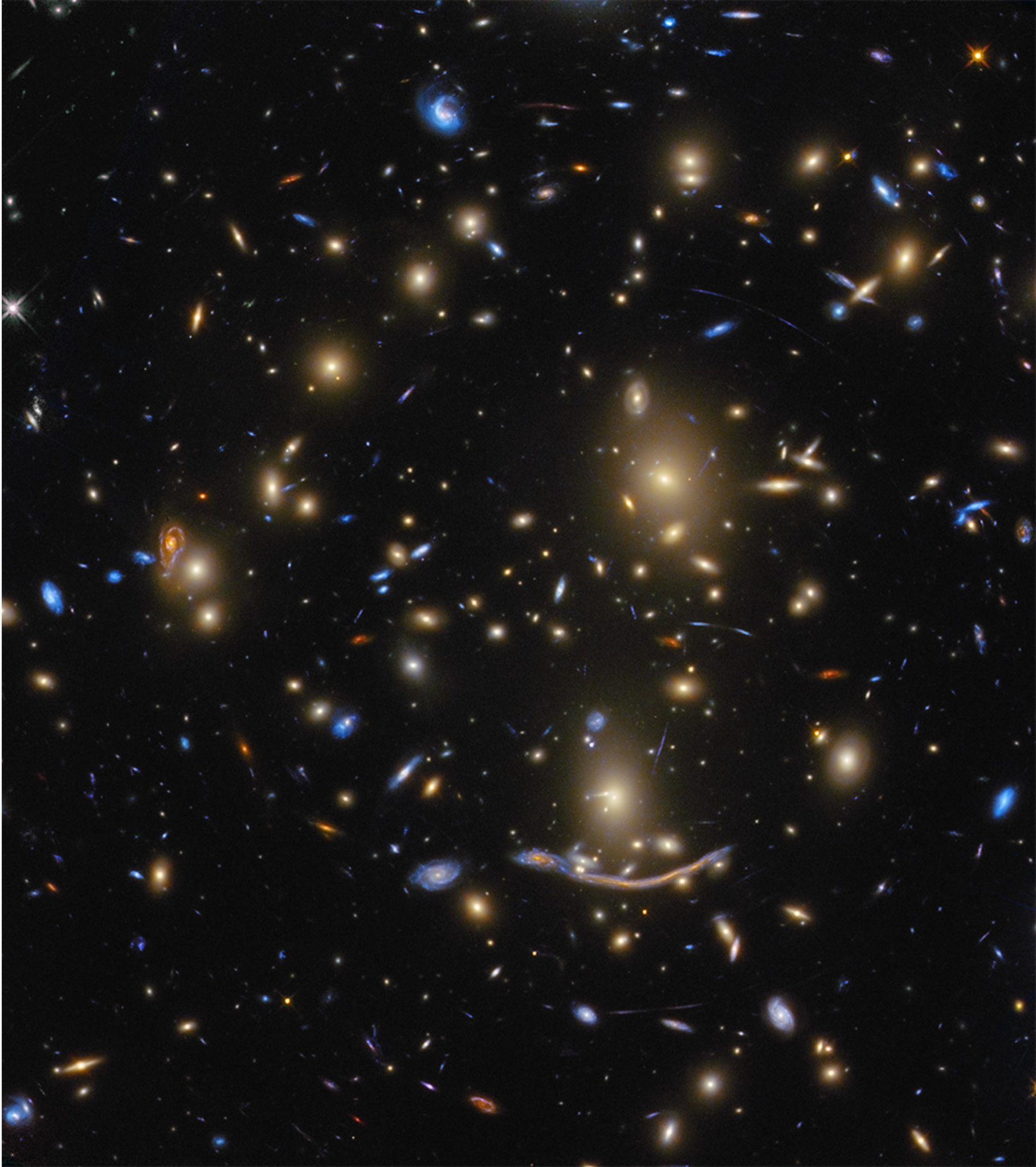
Historical remark: The first gravitational arcs

The first detection of gravitational arcs in galaxy clusters is dated 1986. In this year, two groups independently discovered strongly elongated, curved features around two clusters of galaxies (Soucail et al., 1987; Lynds & Petrosian, 1989): A370 (left panel below) and CL2244-02 (right panel).



They were seen displaced from the cluster center and curving around it. Several hypothesis were put forward about the nature of these features, all proven wrong. The correct interpretation of these observations as gravitational lensing effects was made by Paczynski (1987), when the redshift of the arc in A370 was measured and discovered to be much larger than the redshift on the cluster. In particular, A370 is at redshift $z_d = 0.374$, while the arc is at redshift $z_s = 0.724$. The arc in CL2244-02 ($z_d = 0.3$) is at redshift $z_s = 2.24$. The figures below show color higher quality images





LENS SURVEYS

- CFHT-LS
- Muscles
- Haggles
- Cosmos
- **SLACS**
- **JVAS/CLASS**
- SLS-AEGIS
- OLS
- PANELS
- SOAR
- SGAS
- SDSS
- 2dF Lens Survey
- HST Snapshot Lens Survey
- FKS Lens Survey
- NOT Lens Survey
- APM Lens Survey
- MG Survey
- SARCS
- SBAS
- LoCUSS
- **CLASH**
- **Frontier Fields**

EXAMPLE 1: THE CLASS SURVEY (SOURCE ORIENTED)

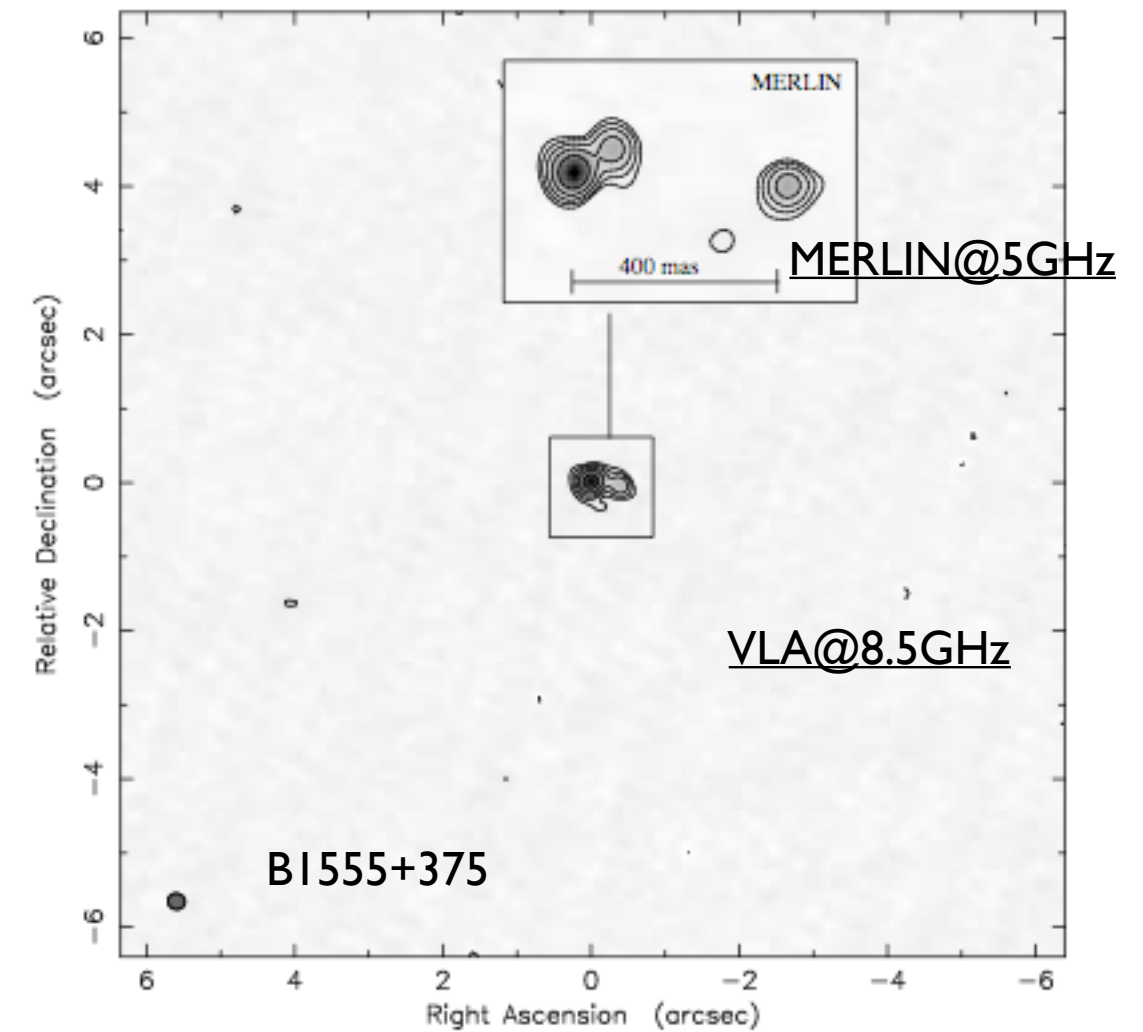
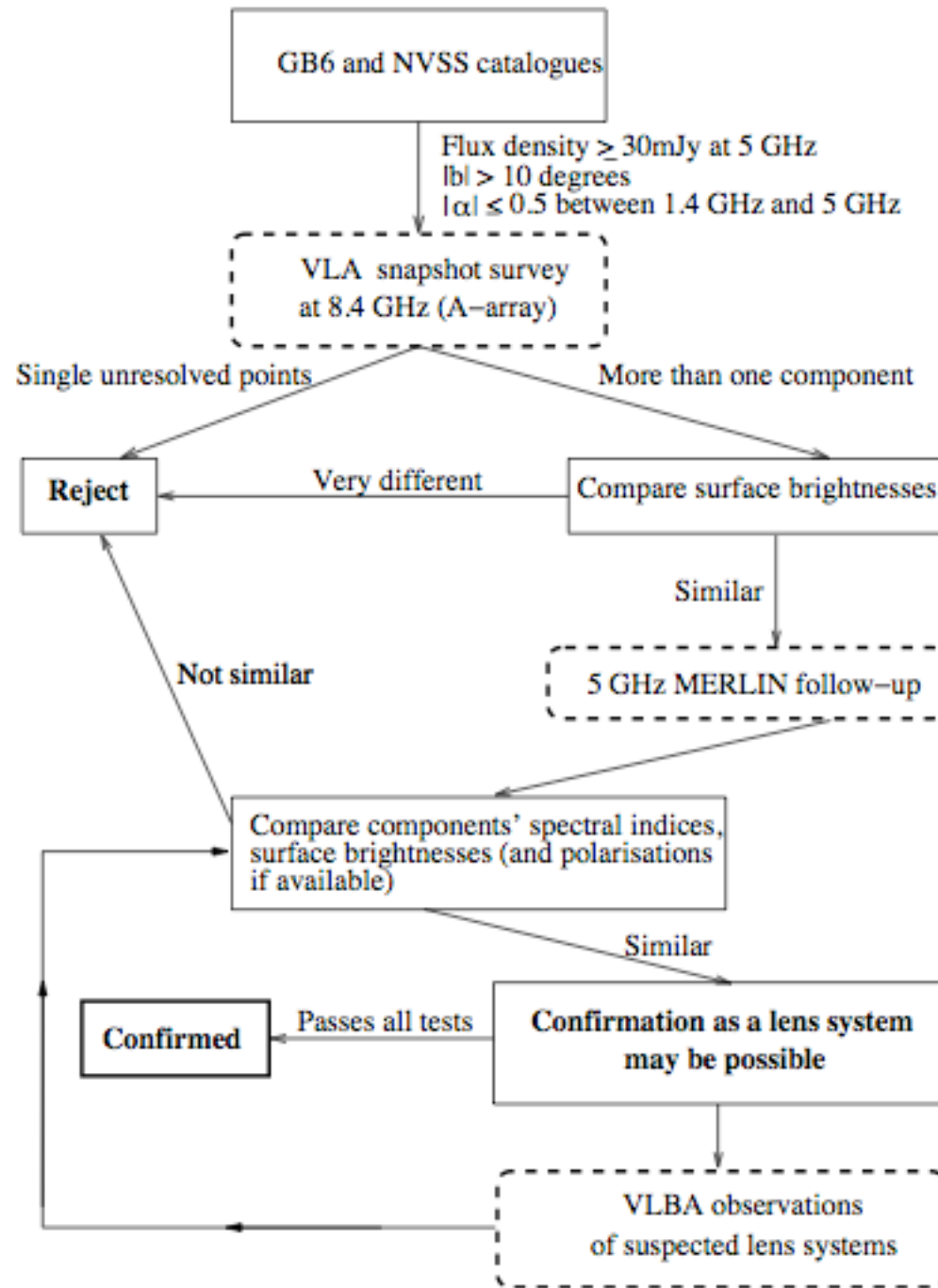
The CLASS (Cosmic Lens All-Sky Survey) was an international project (UK, USA, Netherlands) whose goal was searching for gravitational lenses in the radio domain.

The survey was conducted between 1990 and 1999. During the survey 16503 flat-spectrum radio sources were monitored. Such objects are usually **quasars** and have very **simple radio structures**; they are typically point sources, and occasionally weak extended emission is visible. The point-like radio emission is thought to originate from the base of a relativistic radio jet in an active galaxy, which points more or less at the observer.

The simplicity of these sources is useful for gravitational lensing searches. This is because any flat-spectrum radio source which has extended structure is a possible gravitational lens, as the **extended structure** could represent **multiple images** of a point-like radio source, produced by the gravitational field of an intervening galaxy.

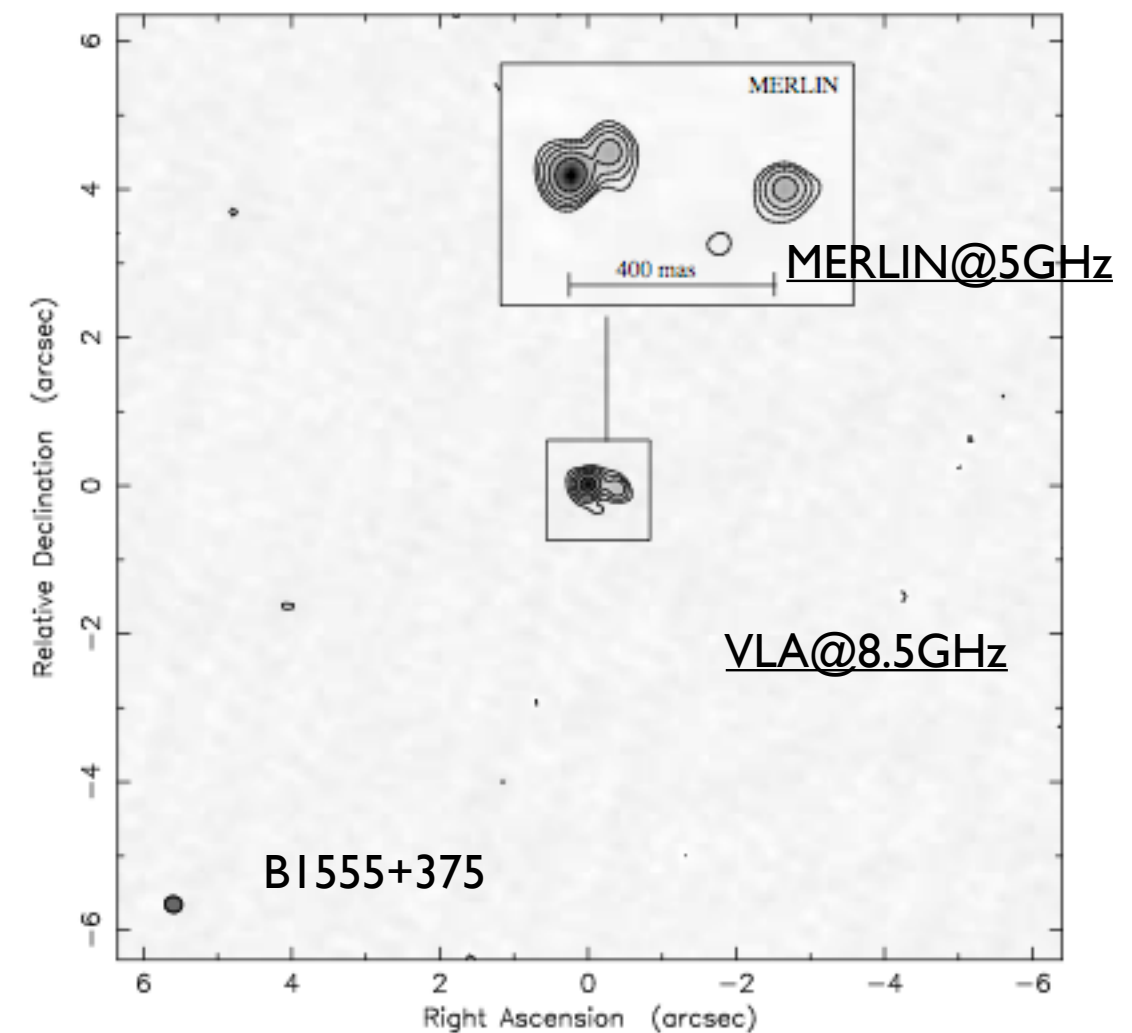
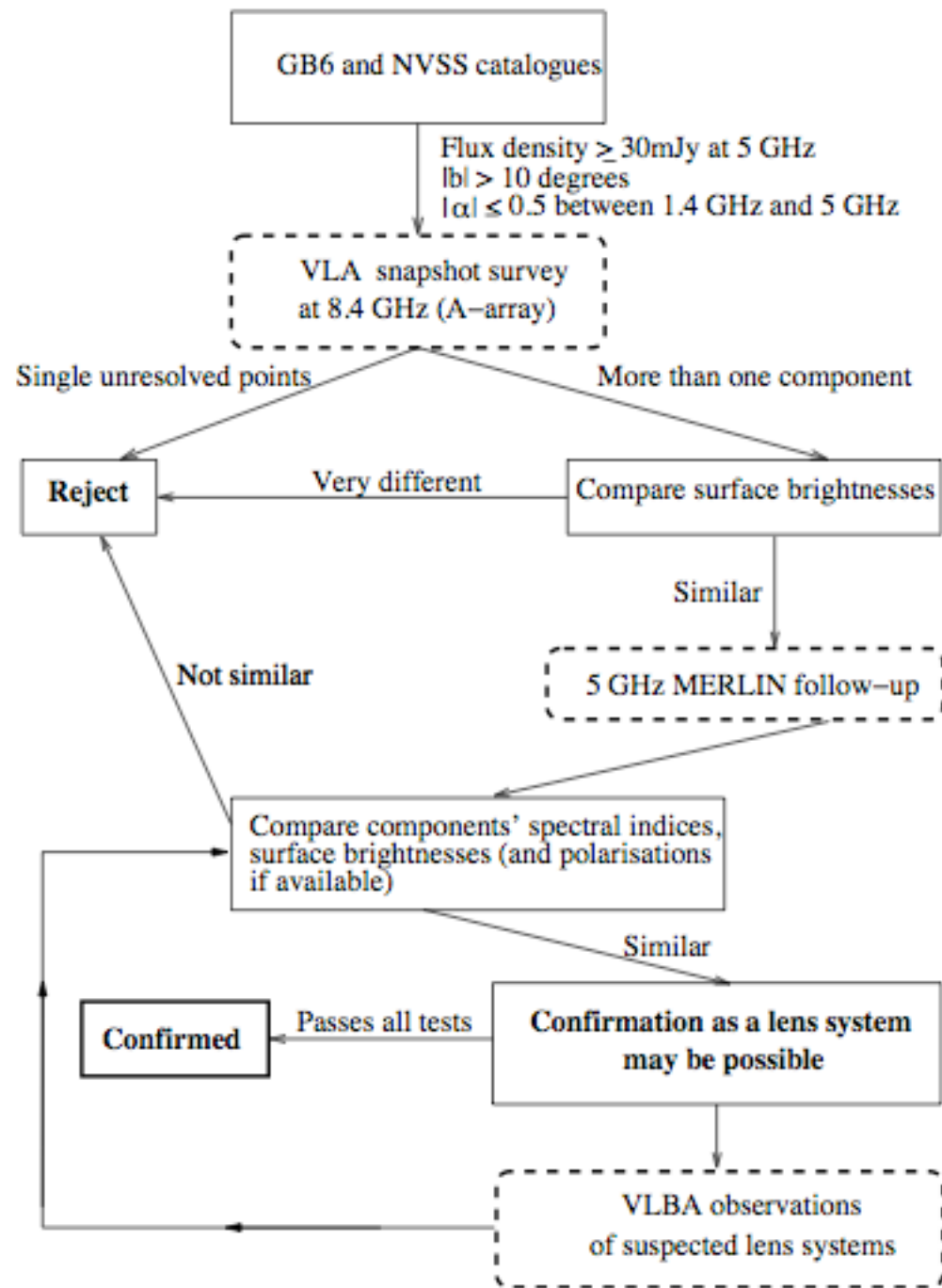
Instruments: VLA (radio maps at 0.2" res.) + follow-up with MERLIN (0.05" res.) and VLBA (0.003" res).

CLASS STRATEGY

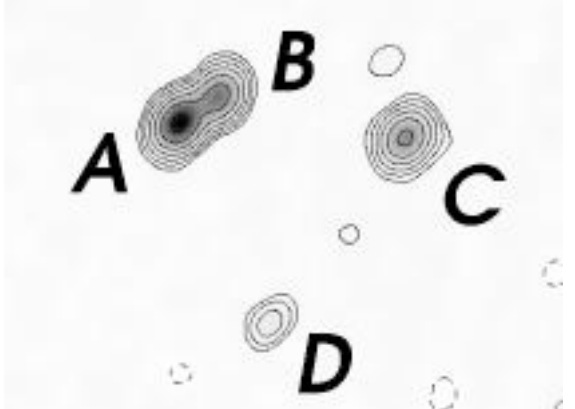


Browne et al. 2002

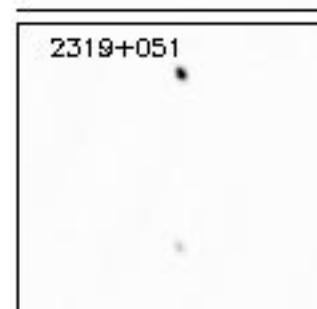
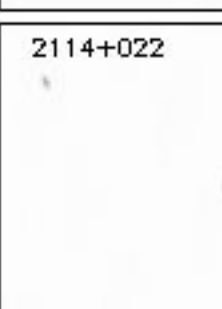
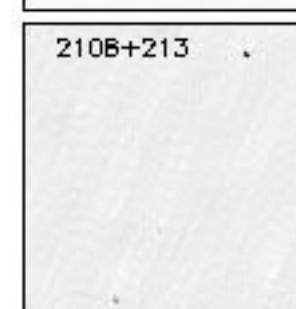
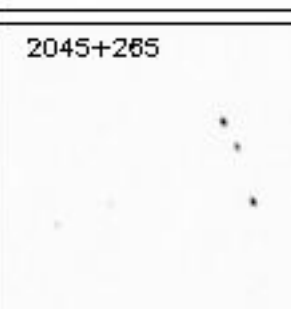
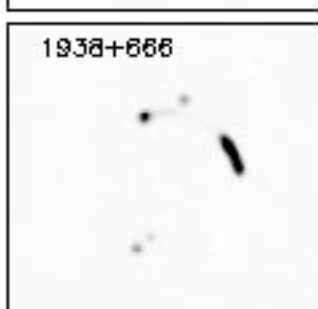
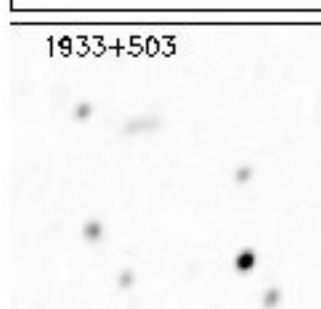
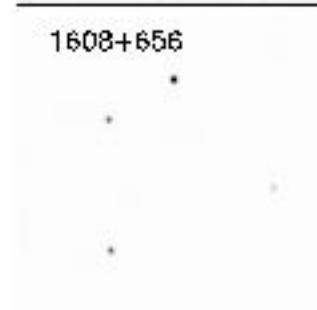
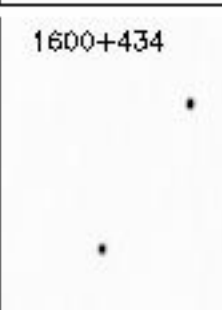
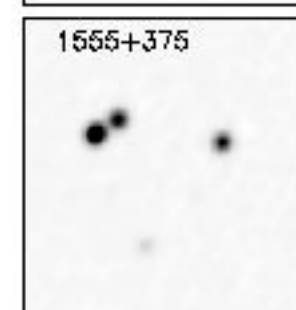
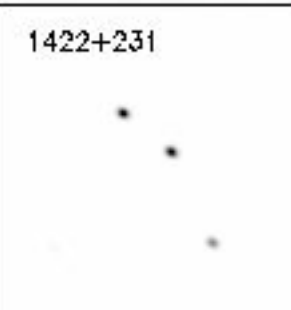
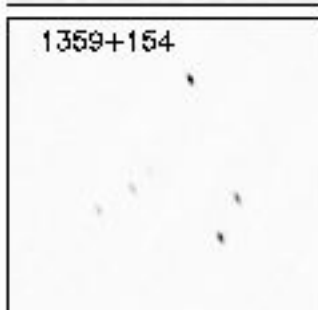
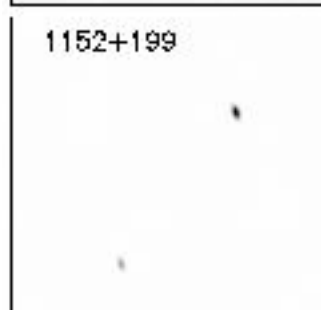
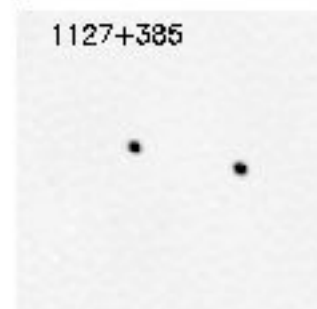
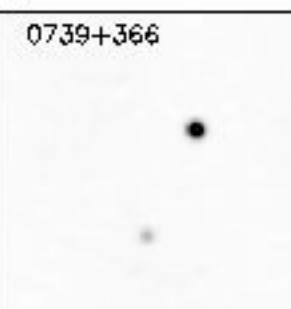
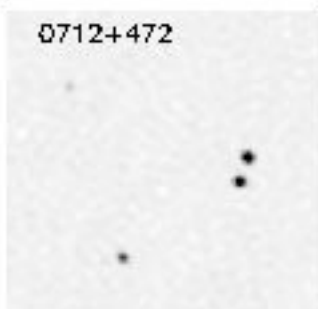
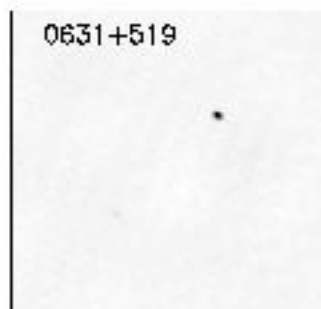
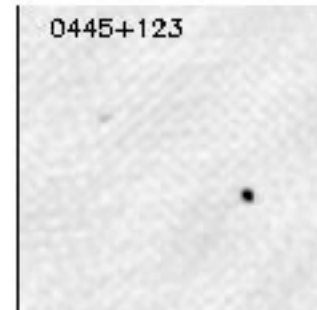
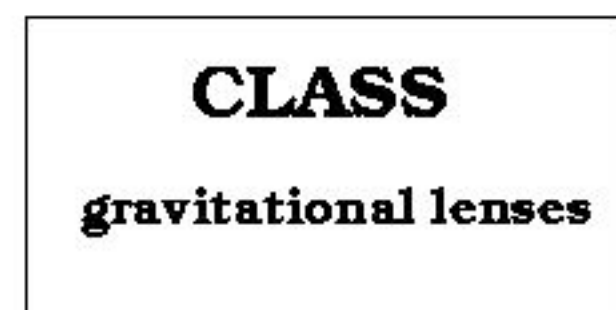
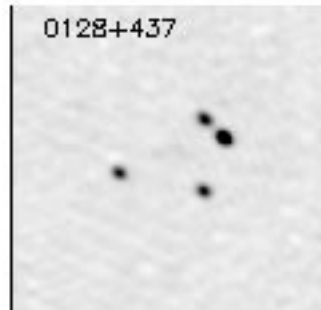
CLASS STRATEGY



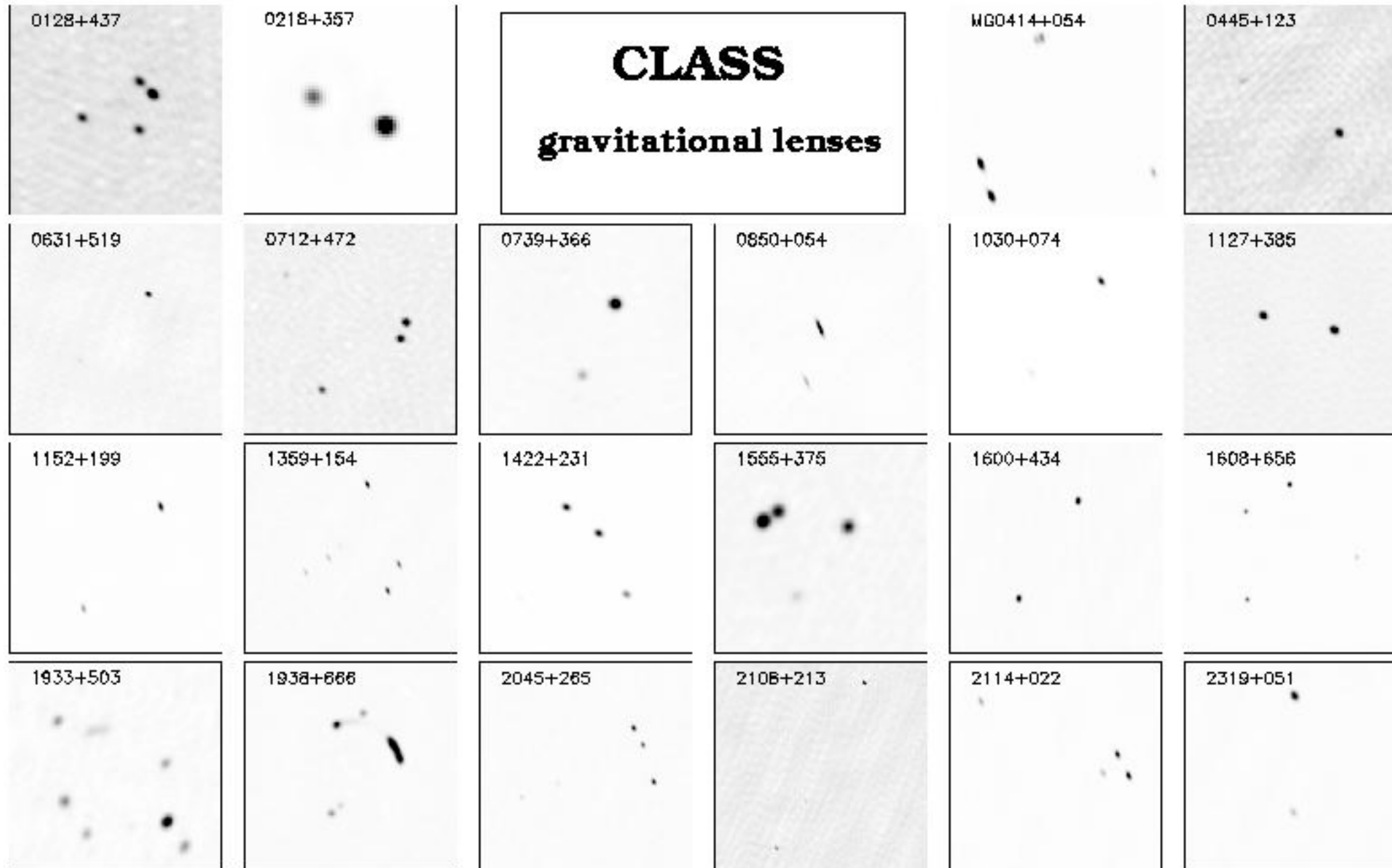
Browne et al. 2002



CLASS LENSES

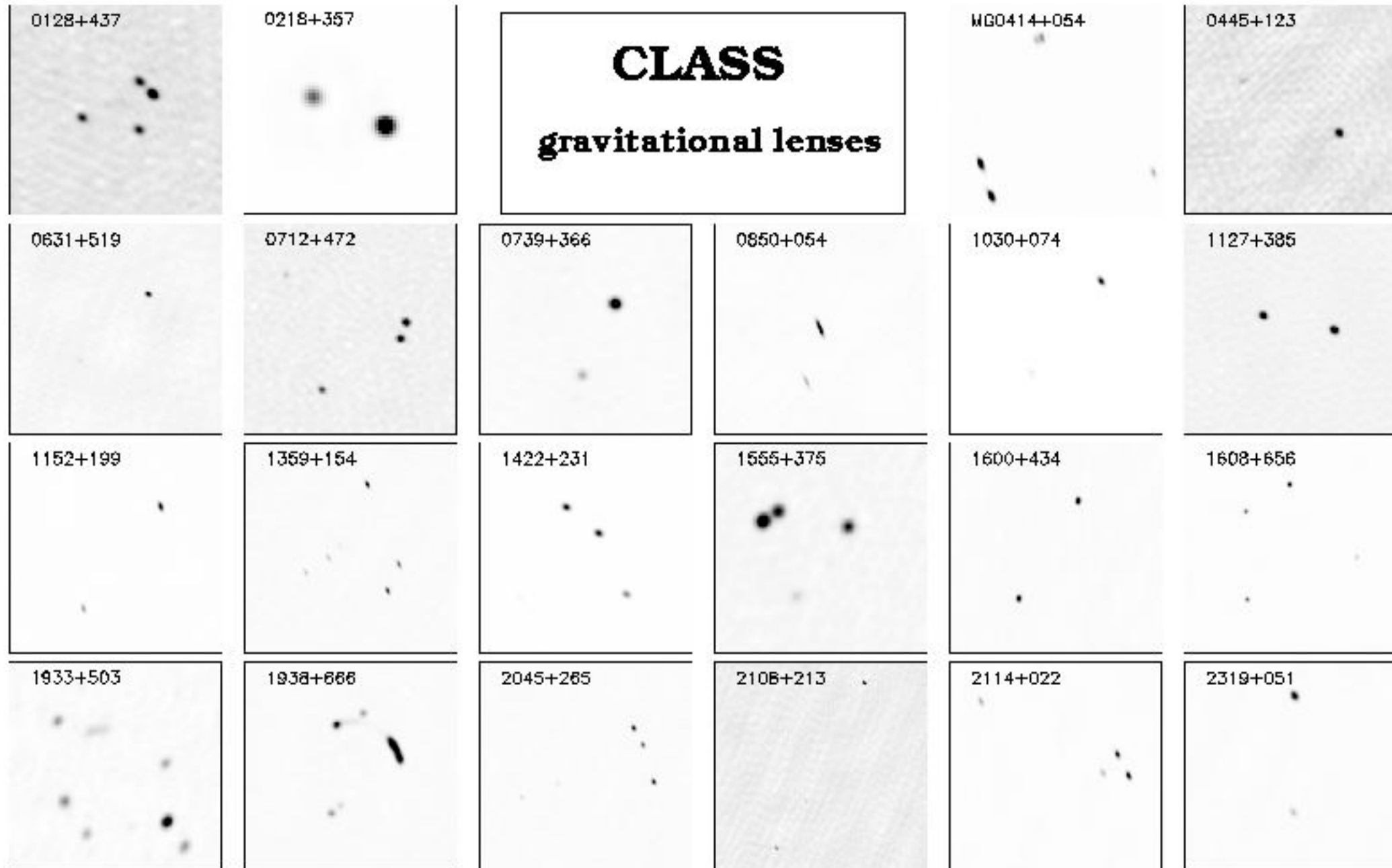


CLASS LENSES



12 double

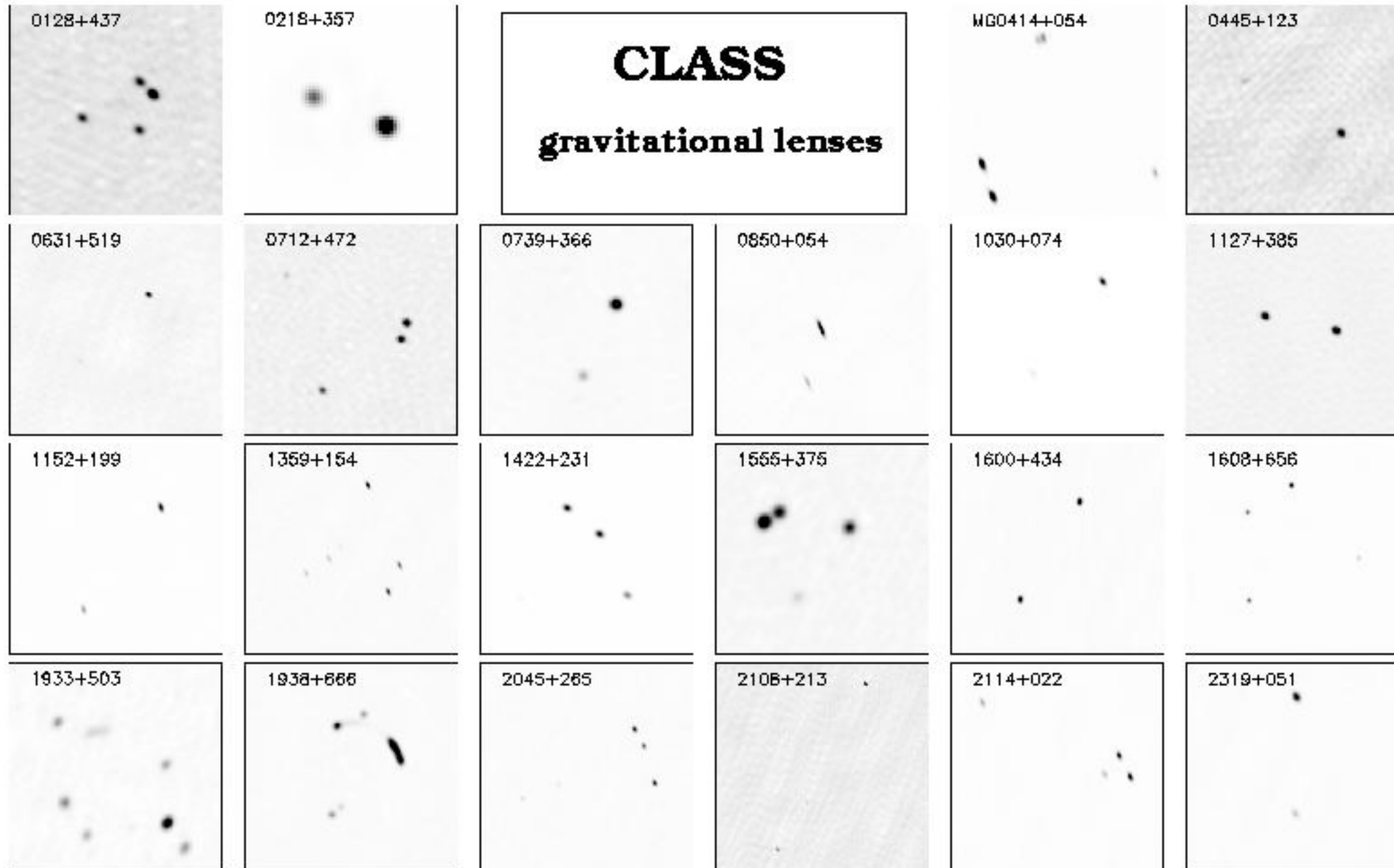
CLASS LENSES



12 double

9 quadruple

CLASS LENSES

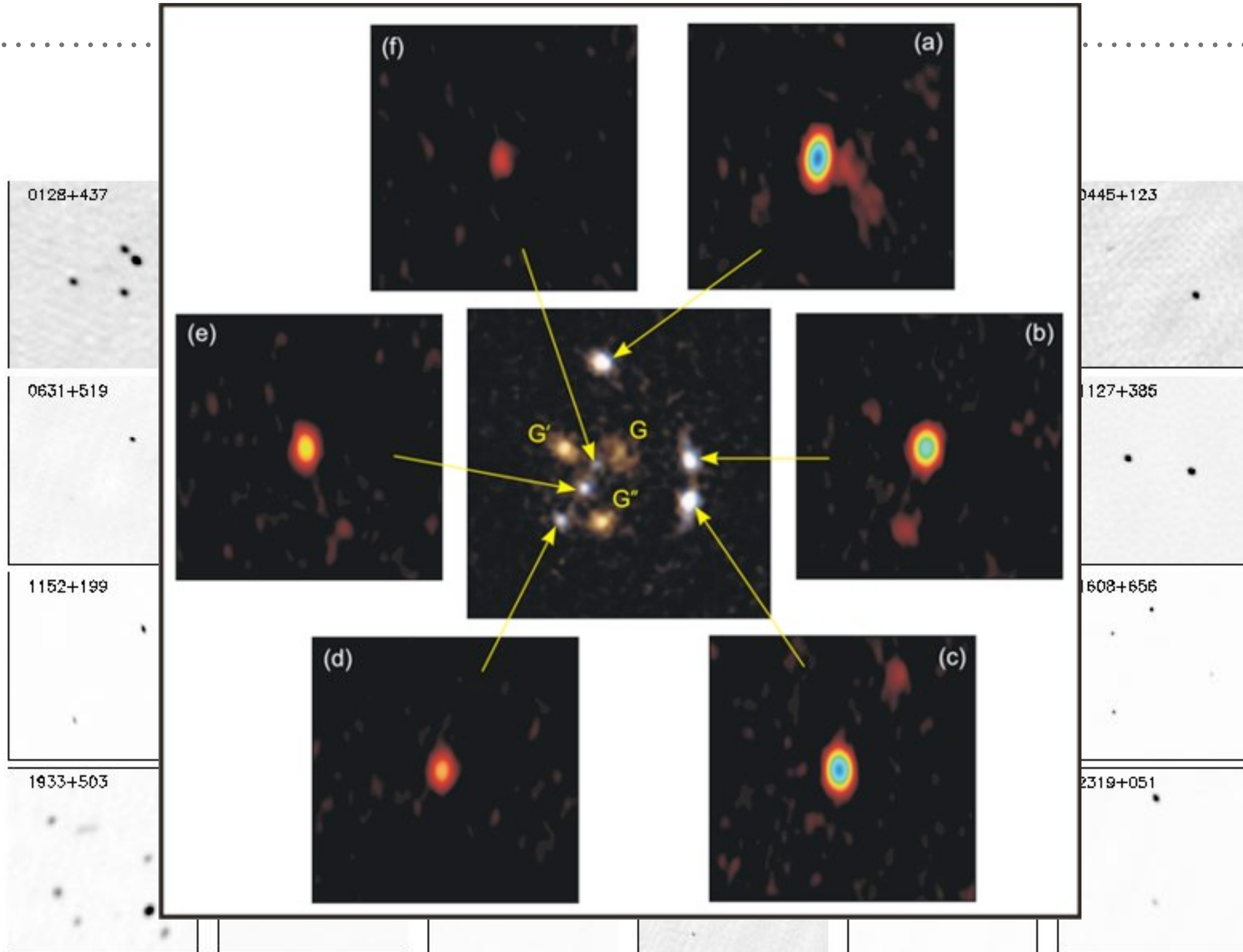


12 double

9 quadruple

1 sextuple

CLASS LENSES



12 double

9 quadrupole

1 sextupole

SLACS (OPTICAL)

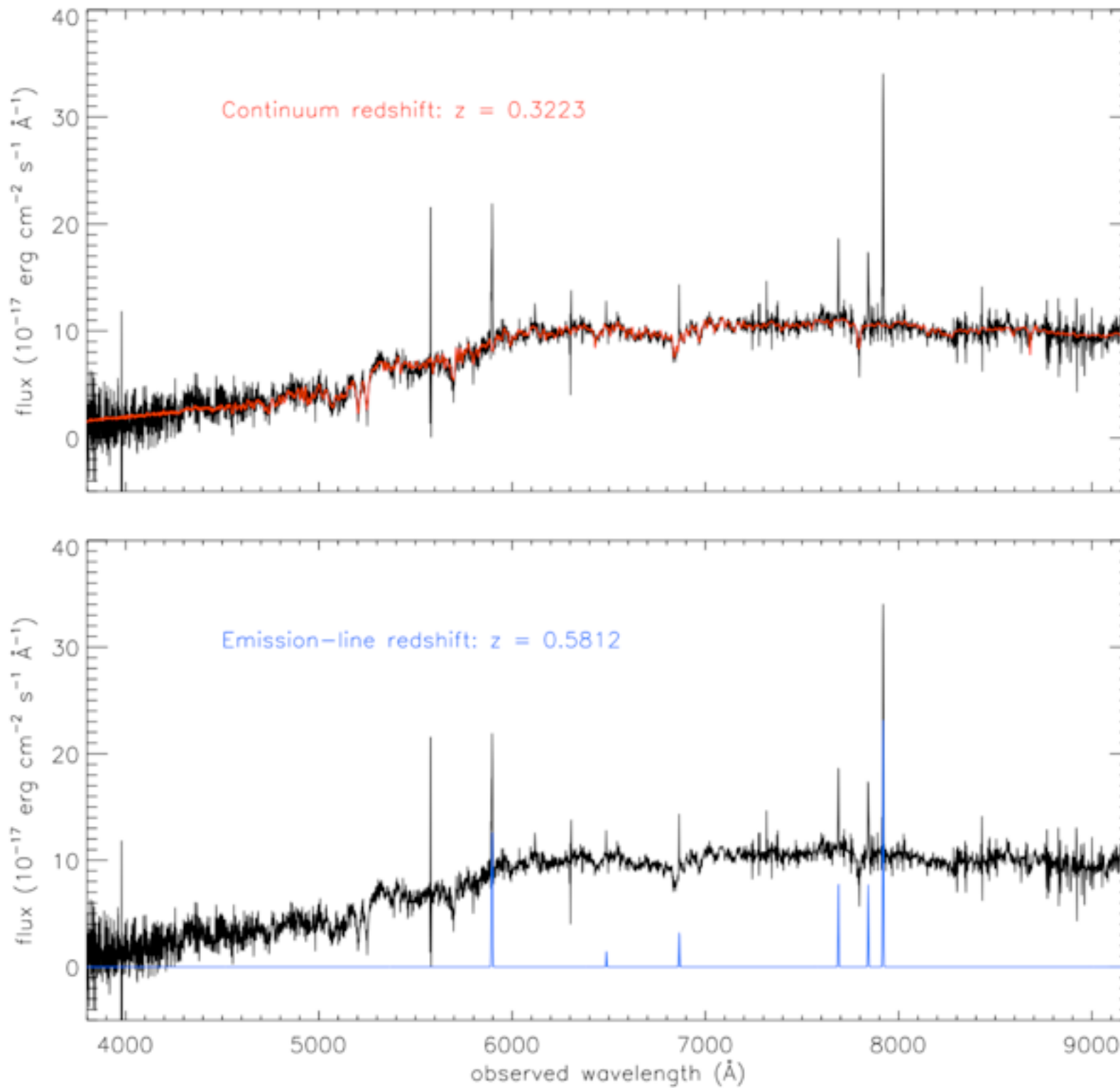
The SLACS (Sloan Lens ACS survey, Bolton et al. 2006) is a very successful project whose goal was finding strongly lensed galaxies behind SLOAN selected galaxies.

The candidate lenses are selected from the spectroscopic database of the Sloan Digital Sky Survey. This survey has produced imaging and spectra for galaxies on a huge portion of the sky (8400 sq. degree). The observations were conducted between 2000-2005 (SDSS-I) and 2005-2009 (SDSS-II) using a dedicated 2.5m-telescope at Apache Point (New Mexico).

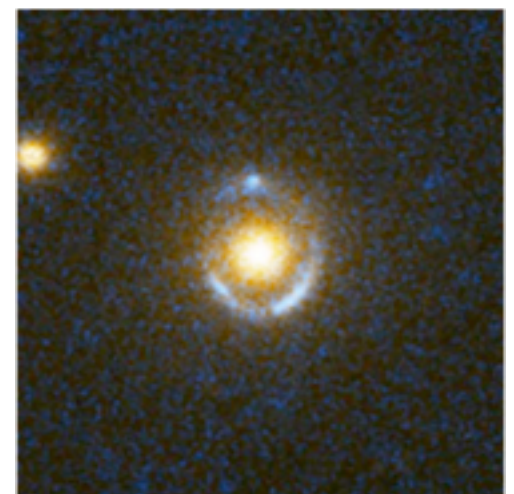
The candidate lenses are galaxies whose spectra can hardly be fitted with a single spectrum. This is an indication of superposition of two different galaxies along the line of sight. This technique follows the discovery of a lens system by Warren et al. (1996)

The selected candidates are observed at high-resolution with the ACS onboard HST.

SLACS STRATEGY

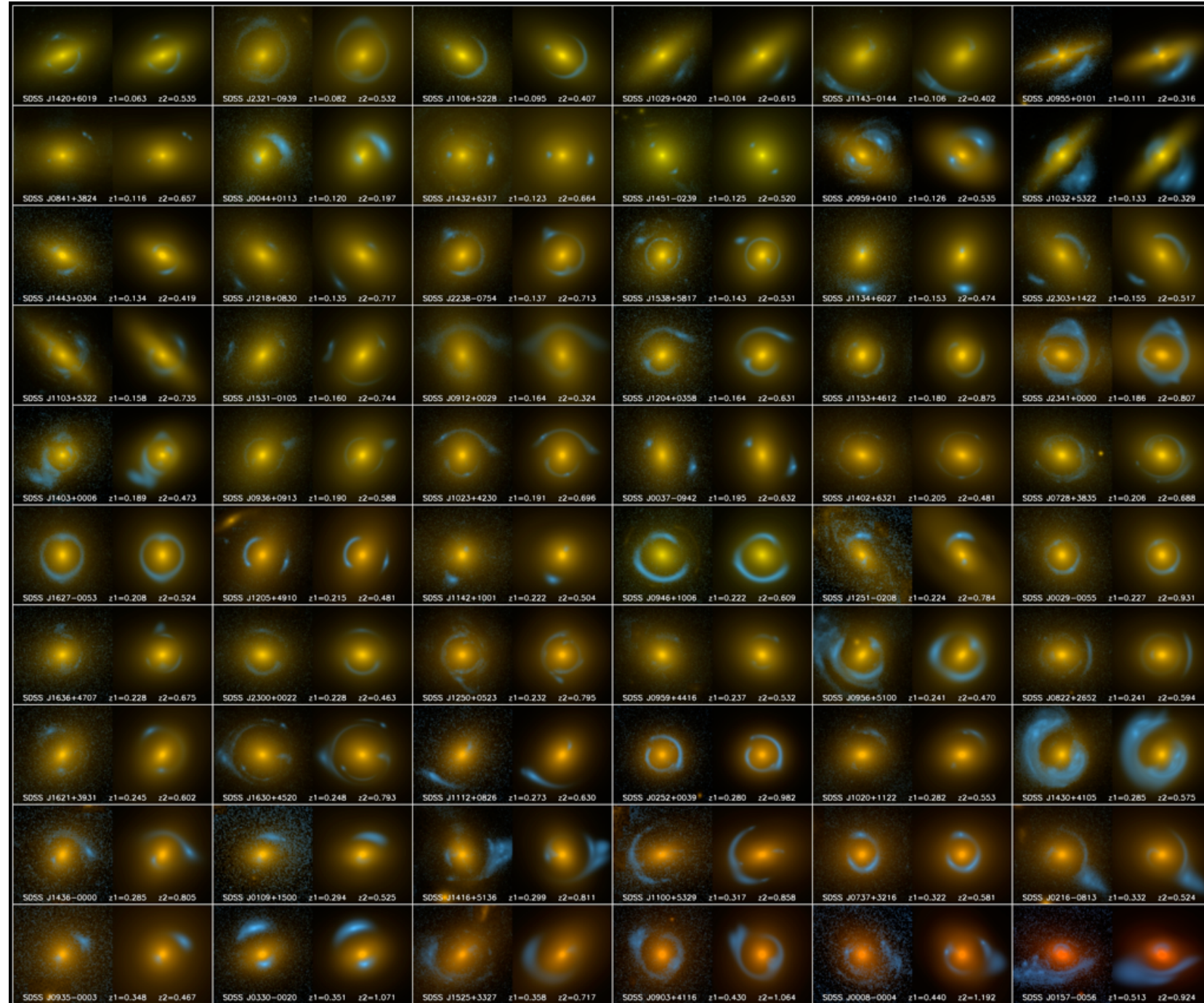


SLOAN image



HST follow-up

SLACS LENSES



SLACS: The Sloan Lens ACS Survey

A. Bolton (U. Hawai'i IfA), L. Koopmans (Kapteyn), T. Treu (UCSB), R. Gavazzi (IAP Paris), L. Moustakas (JPL/Caltech), S. Burles (MIT)

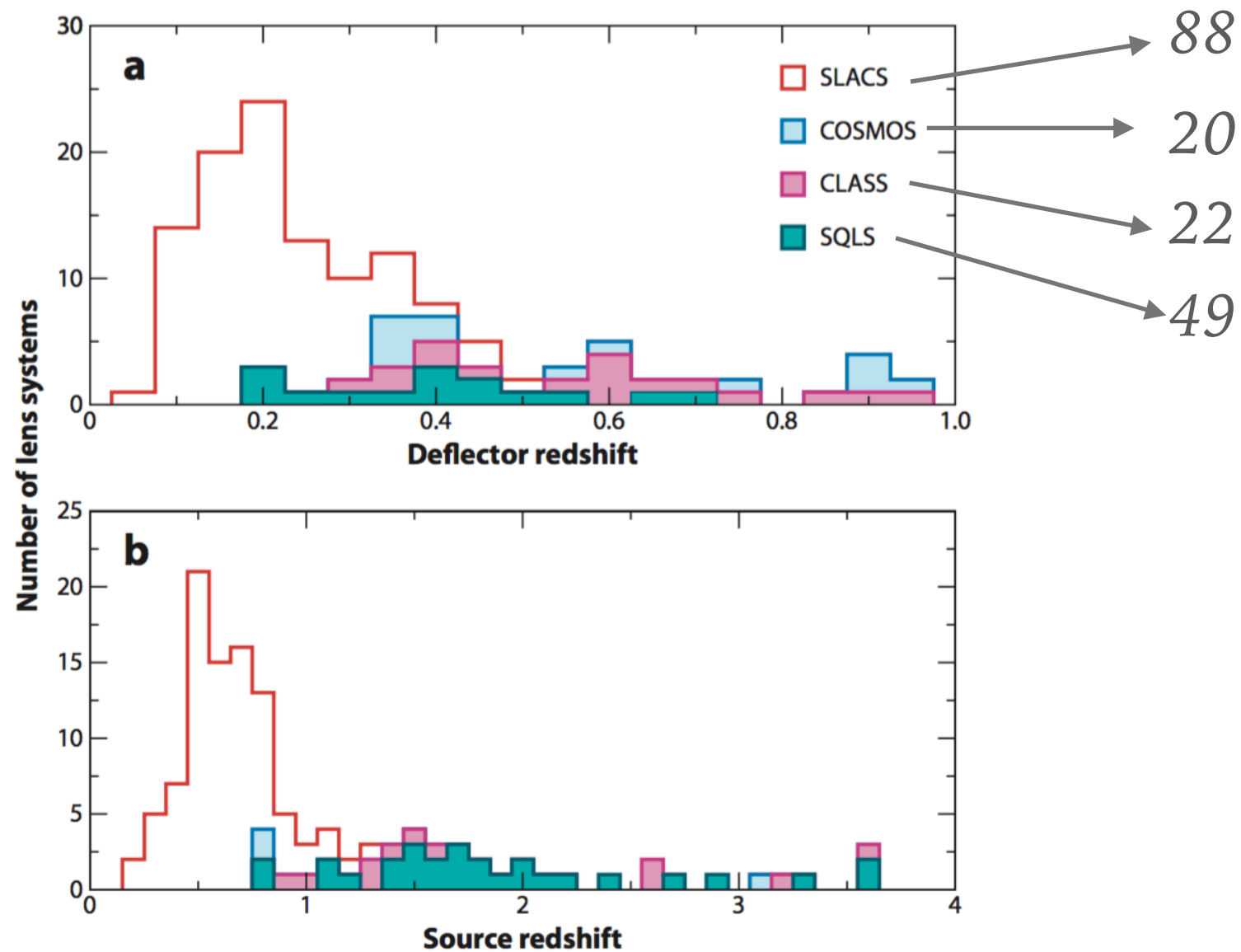
www.SLACS.org

Image credit: A. Bolton, for the SLACS team and NASA/ESA

- 85 galaxy lenses
- 13 probable lenses
- redshifts for all systems
- 80% ellipticals
- 10% lenticular
- 10% spirals (mostly bulge dominated)
- big galaxies with v. disp.
~200-300 km/s (average:
248 km/s)

CURRENT STATE OF THE ART

- ~250 galaxy strong lenses (secure; source www.masterlens.org)
- ~80 galaxy clusters (mainly found by visually inspecting ground based imaging data or HST WFC2/ACS/WFC3 images)



WE ENTERED A NEW ERA: AUTOMATED SEARCHES FOR LENSES

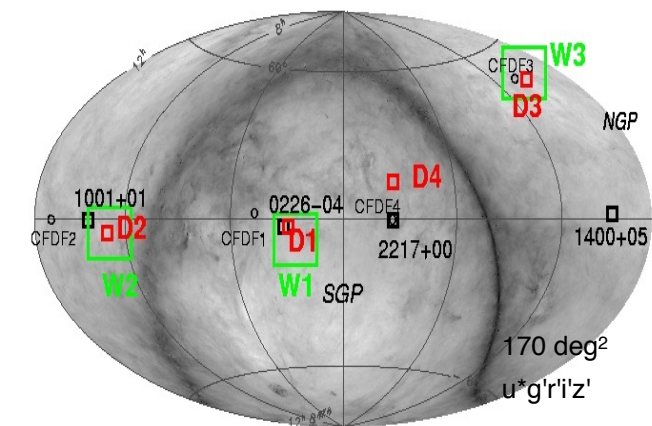
- Recently, some imaging surveys begun covering large areas of the sky with good depth and good spatial resolution
- These surveys were proposed mainly as cosmological experiments employing weak lensing
- Despite their main goal, the data are of good quality also to exploit strong lensing
- The strategy had to be changed: large areas, big depth, large number of potential lenses, making difficult the lens identification via visual inspection.
- The idea of “automated detection” took place

AN EXAMPLE: THE SL²S SURVEY AND THE “RINGFINDER”

- CFHTLS: 150 sq. deg.; I<24.5; sub arcsec PSF; 640.000 potential lenses (ETGs) to be searched for SL features (Strong Lensing Legacy Survey, SL²S)
- u,g,r,i,z

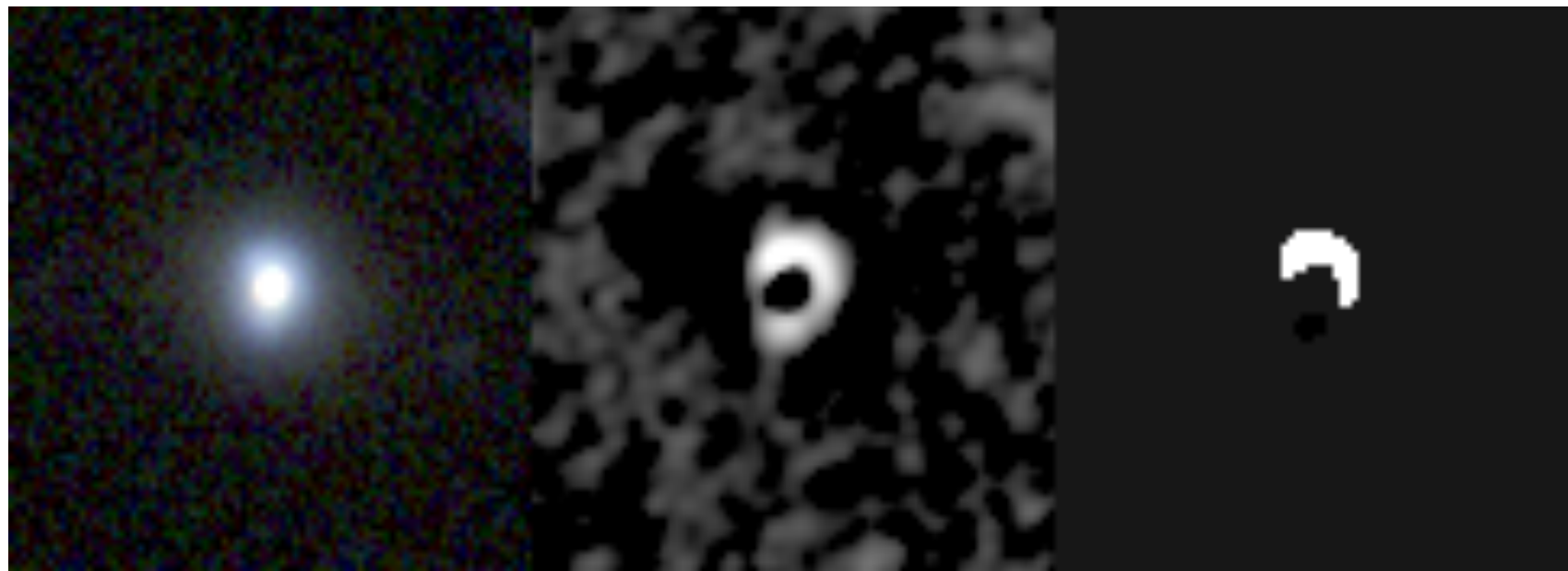


**Wide
Survey**



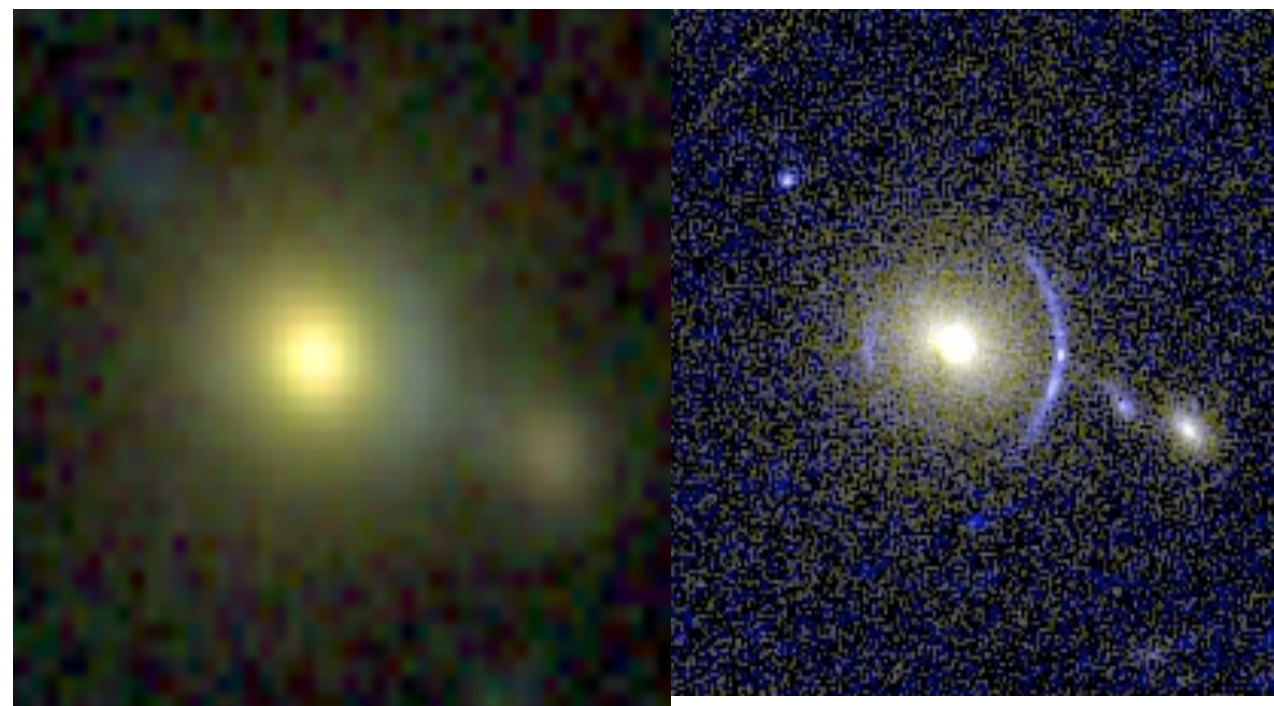
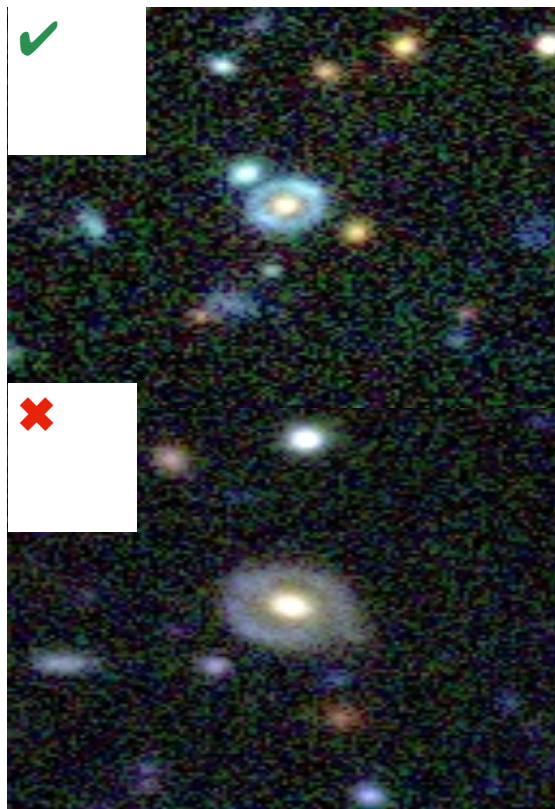
AN EXAMPLE: THE SL2S SURVEY AND THE “RINGFINDER”

- RingFinder (Gavazzi, 2012): a software to search for blue star forming faint blobs, tangentially elongated around ETGs
- Efficient lens light subtraction: $g-\lambda i$, tune λ to remove the ETG
- Scan the image, looking for tangentially elongated blue residuals
- Processing time 2 CPU weeks for 150 sq. deg.



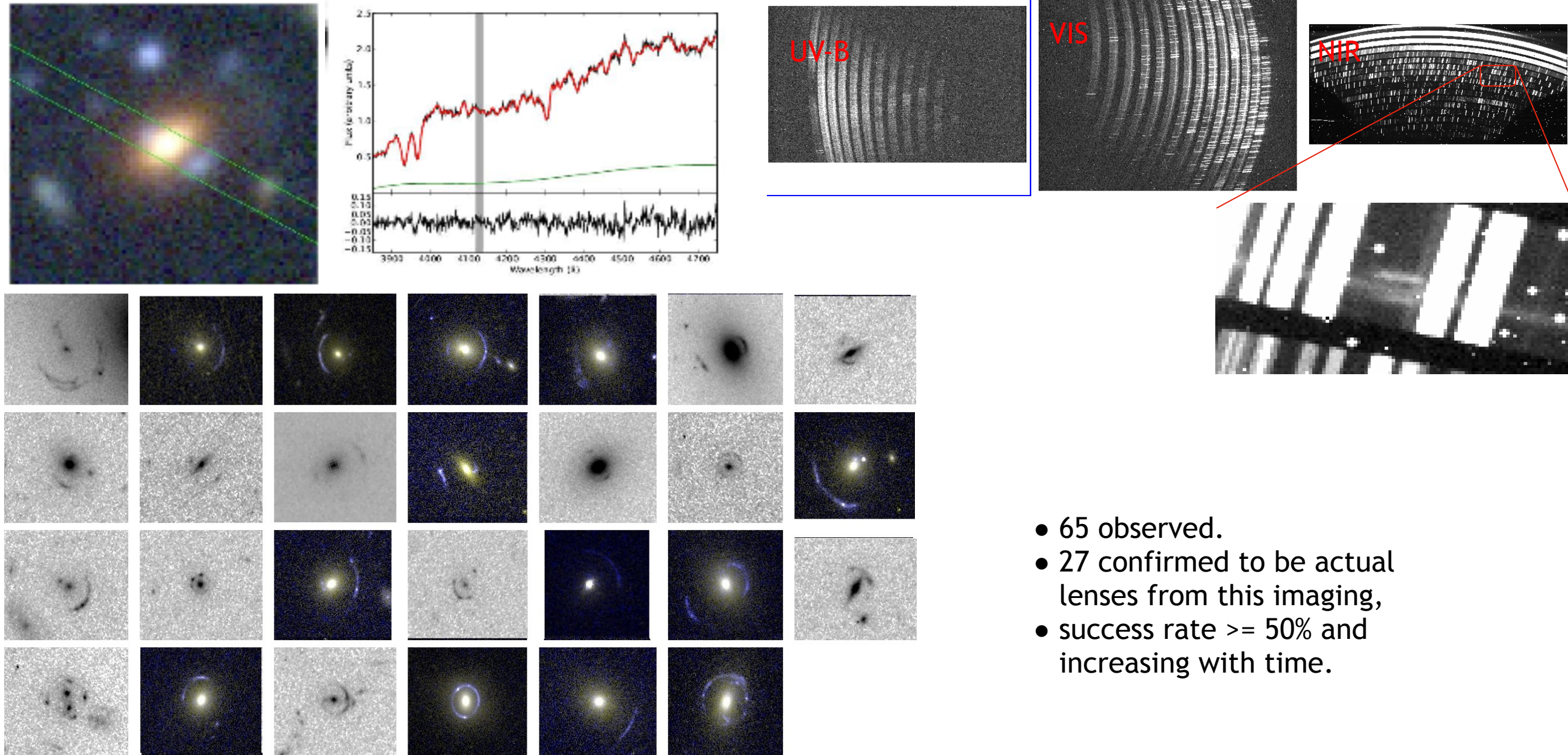
AN EXAMPLE: THE SL2S SURVEY AND THE “RINGFINDER”

- Followed by visual inspection to remove false positives (mainly polar ring galaxies)...
- ...HST follow-up...



AN EXAMPLE: THE SL2S SURVEY AND THE “RINGFINDER”

- ... and spectra (VLT-XShooter (19); Keck/LRIS (46))

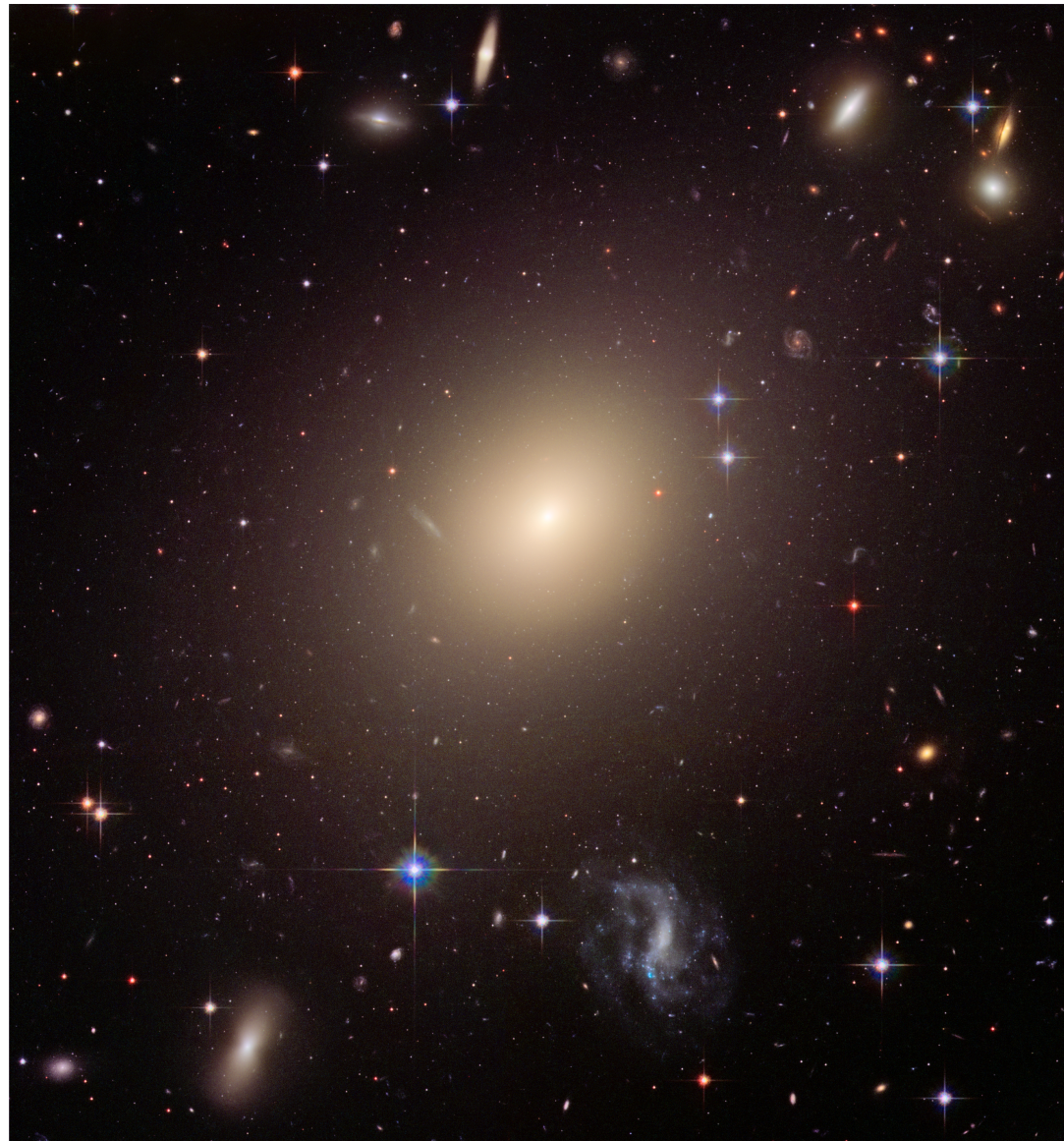


THE FUTURE: MACHINE LEARNING

- Machine learning techniques to classify lenses/non lenses (supervised/un-supervised)
- Several classification algorithms can be successfully used to find gravitational lenses within large surveys
- Deep learning
- Some promising techniques:
 - convolutional neural networks
 - SVM
 - ...

GALAXIES AND CLUSTERS AS LENSES

Elliptical galaxies



ESO 325-G004

- ellipsoidal/spheroidal shape
- light follows Sersic profile with $n=4$ or larger
- sustained by velocity dispersion
- large range of masses: 10^7 - $10^{13} M_{\odot}$
- poor gas content
- no or very limited star formation; old stellar populations
- red colors
- most frequent in dense environments

GALAXIES AND CLUSTERS AS LENSES

spiral galaxies

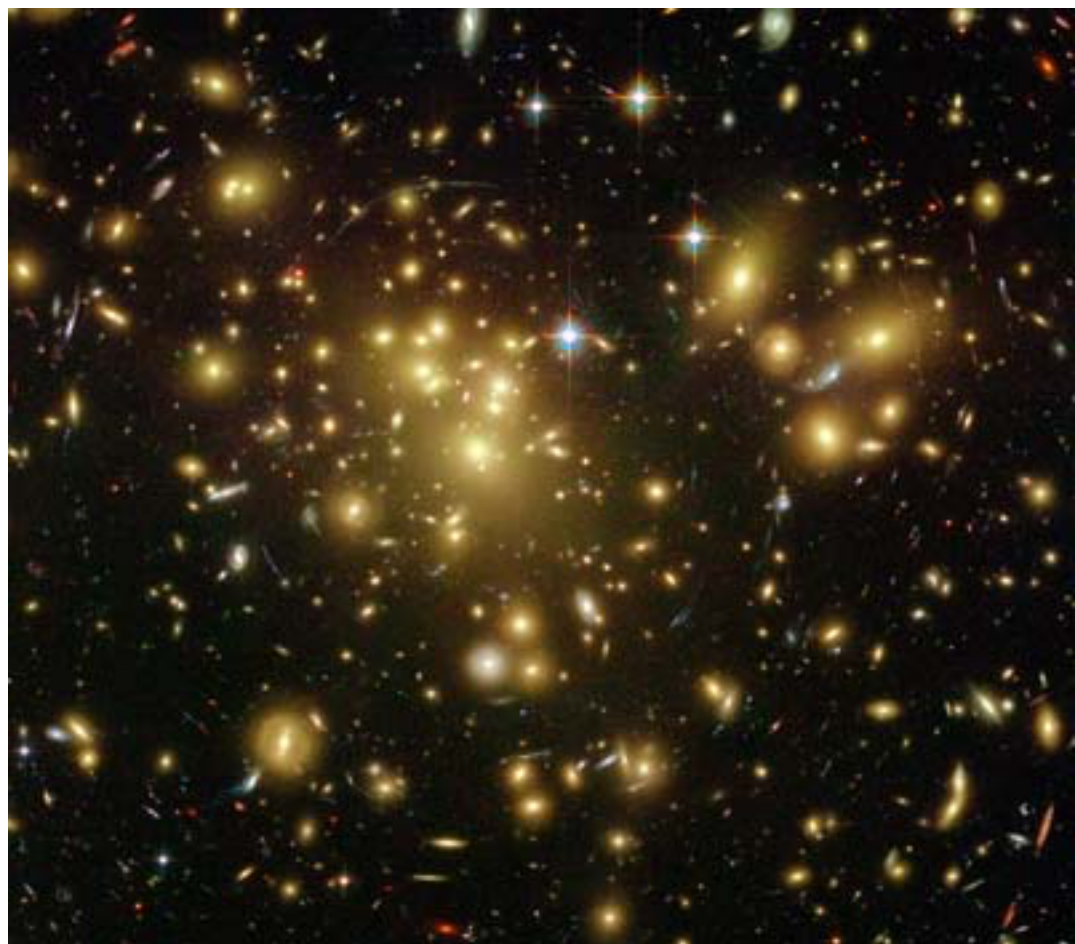


NGC 1300 / NGC 5457

- disk + bulge (+ bar)
- light follows Sersic profile with $n=4$ or larger in bulges; $n \sim 1$ in disks
- disks sustained by rotation
- large range of masses: $10^9 - 10^{12} M_\odot$
- rich of gas and dust
- active star formation in the disk
- red bulges/ blue disks
- most frequent in the field

GALAXIES AND CLUSTERS AS LENSES

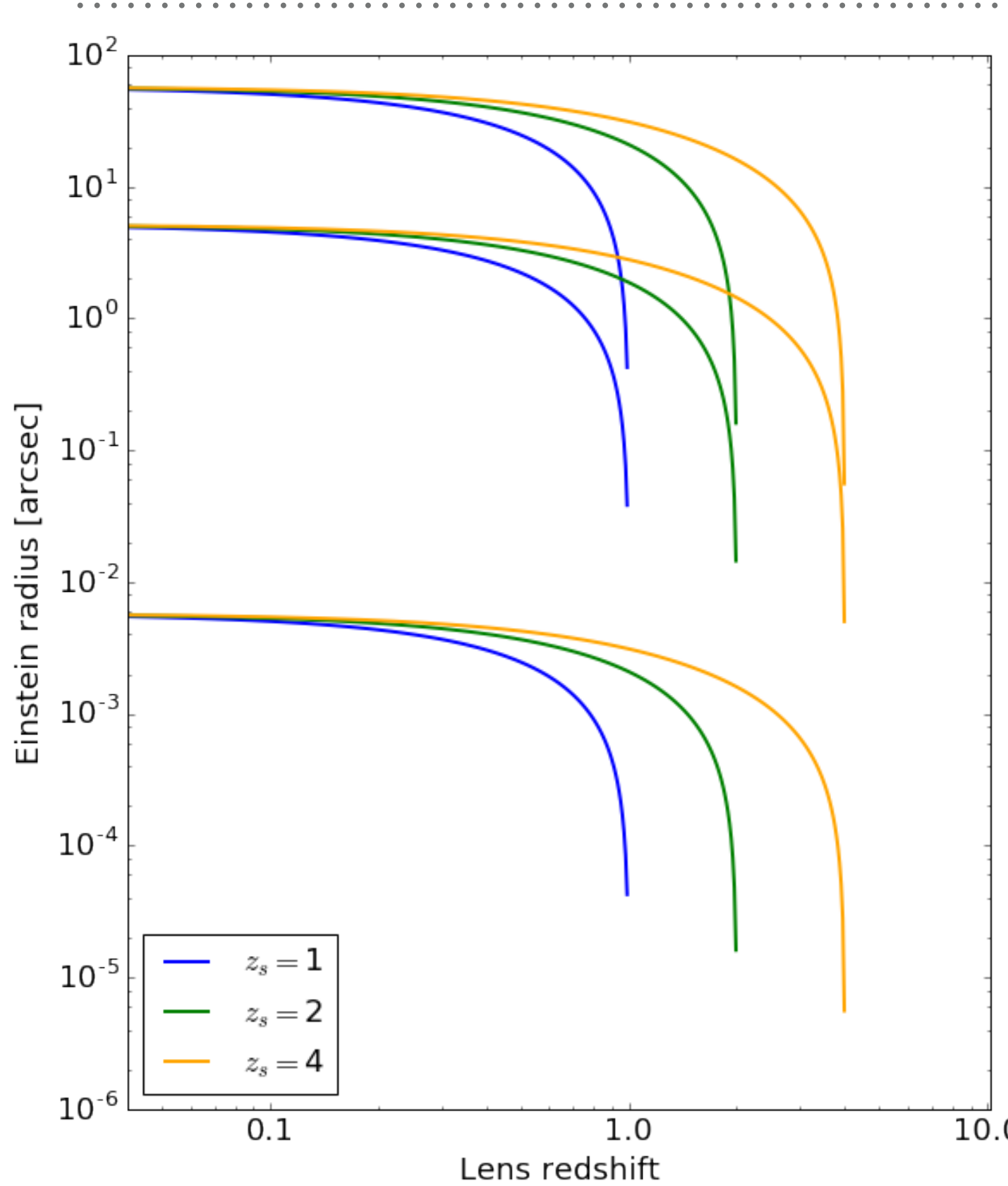
galaxy clusters



Abell 1689

- largest bound cosmic structures
- tail of the mass function:
 $10^{13}\text{-}10^{15}M_{\odot}$
- 11-12% gas; $\sim 1\%$ stars
- contain thousands of galaxies
- red sequence of elliptical galaxies + blu cloud of spiral galaxies

SIZES OF THE EINSTEIN RADII



Galaxy cluster (1000 km/s)

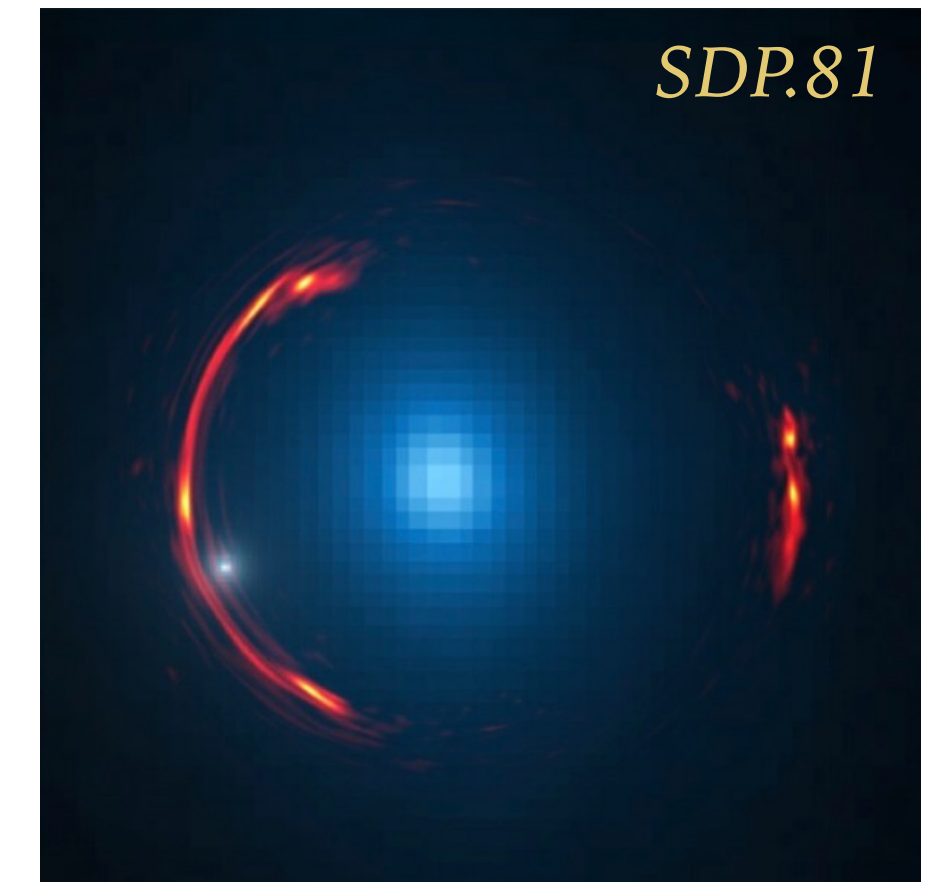
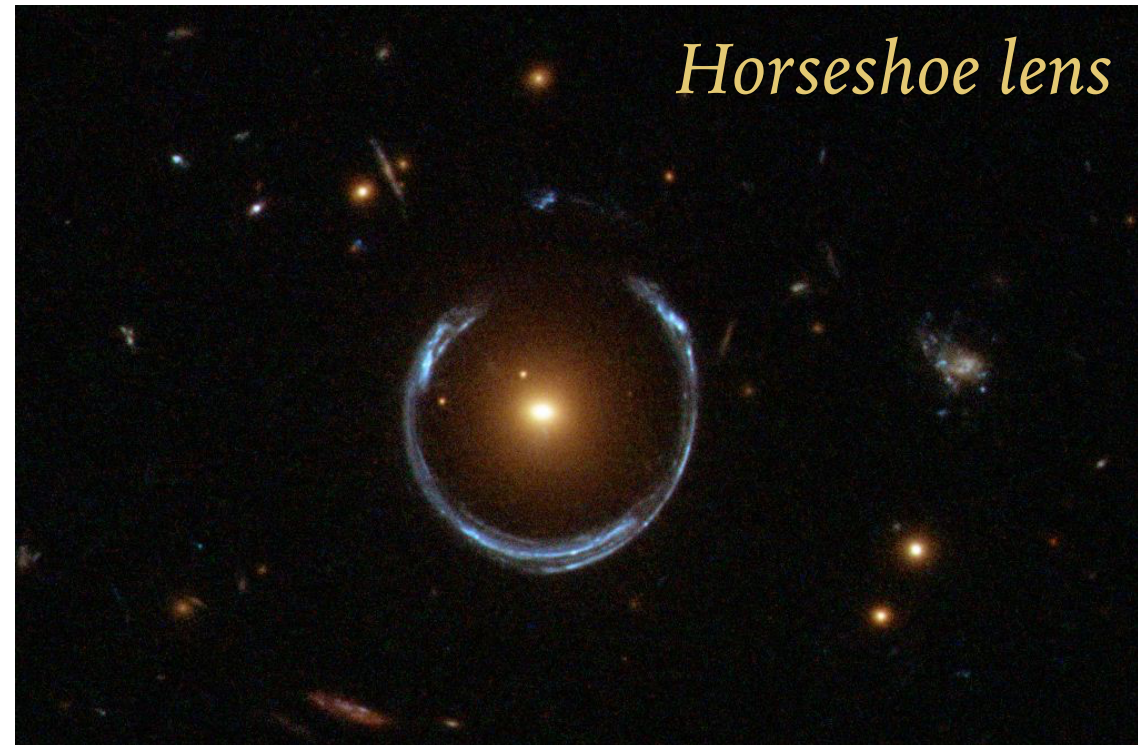
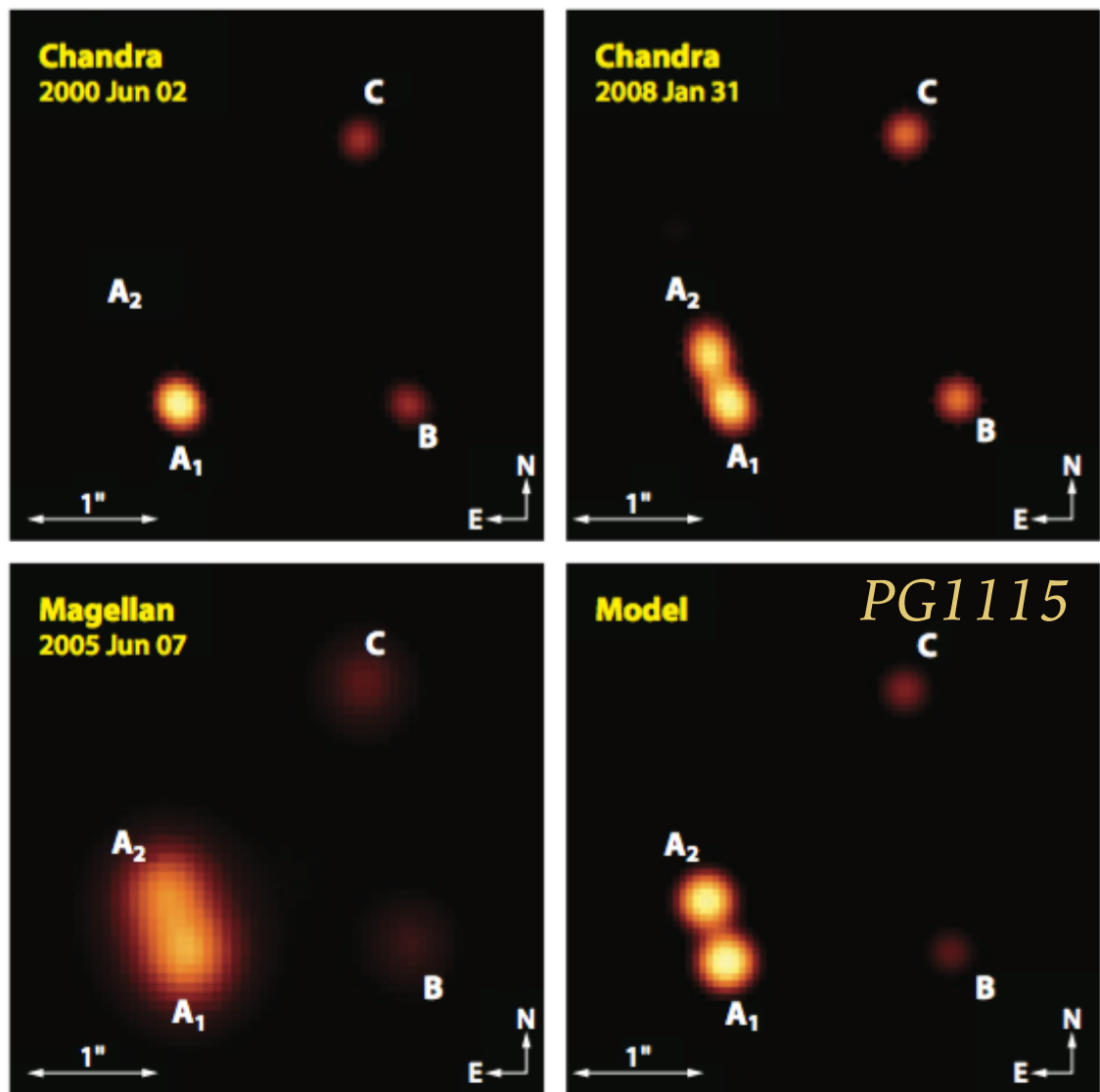
Massive elliptical (300 km/s)

Dwarf satellite (10 km/s)

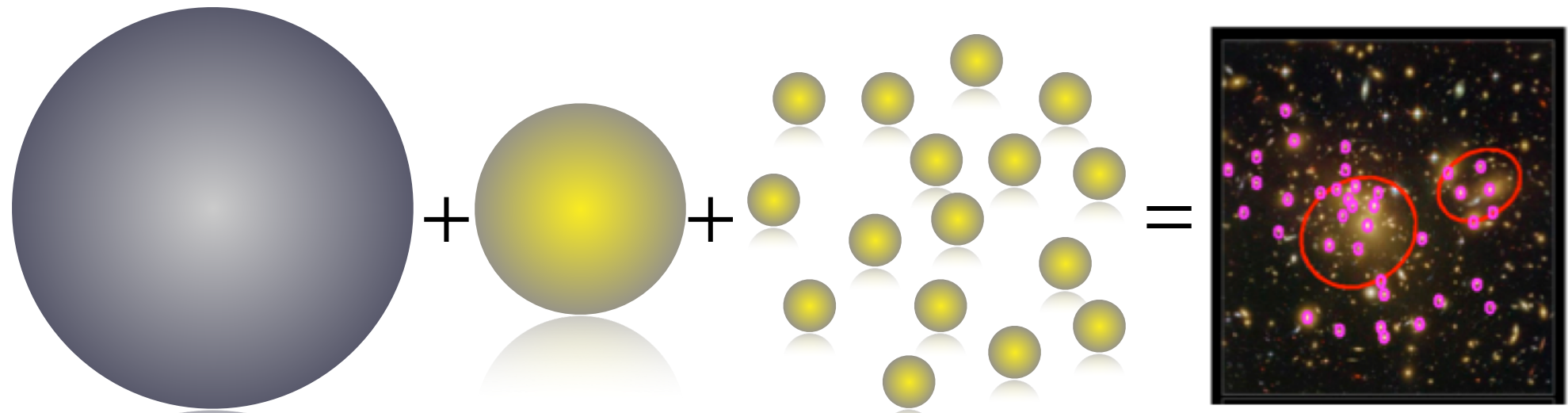
Stars

MULTIPLE COMPONENTS – MULTIPLE LENSING REGIMES

- macrolensing: the dark matter halo, galaxies
- millilensing: substructures in galaxies
- microlensing: stars in galaxies

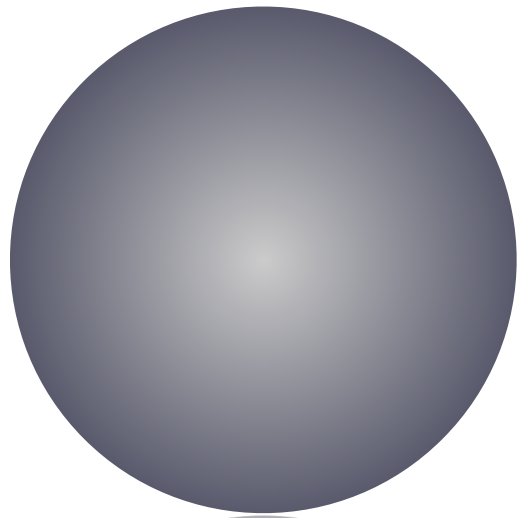


LENS MODELING: THE PARAMETRIC APPROACH



- lenses as complex mass distributions (DM+baryons)
- use stars to trace mass $\mathbf{[x_c]}$
- smooth halo + clumpy structure

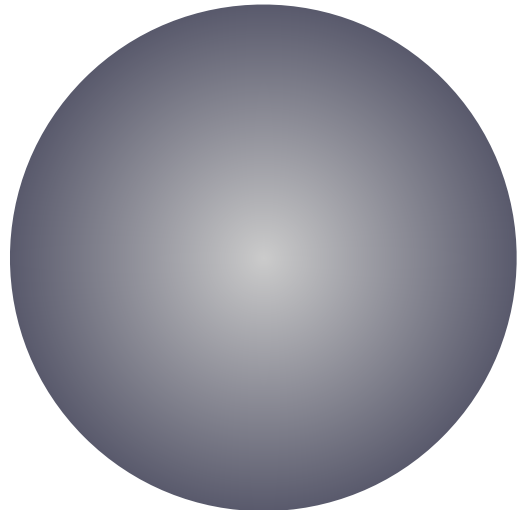
SMOOTH COMPONENT (AND MOST IMPORTANT SUBSTRUCTURES)



[**q**] [**m**]

density prof. *shape*

SMOOTH COMPONENT (AND MOST IMPORTANT SUBSTRUCTURES)

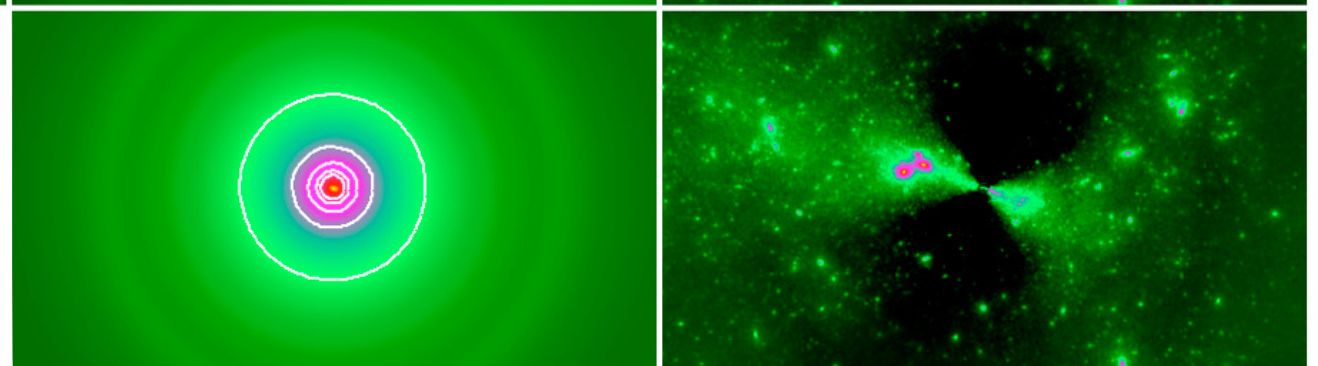
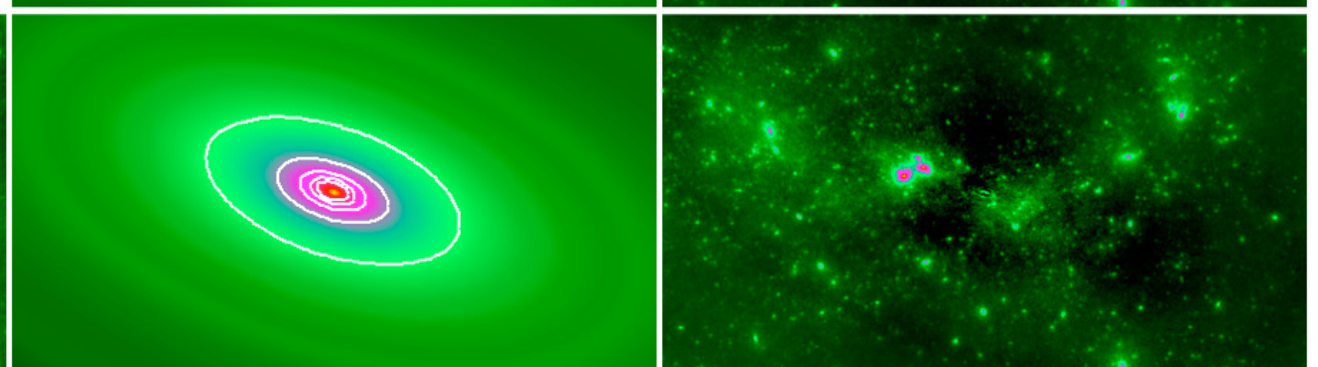
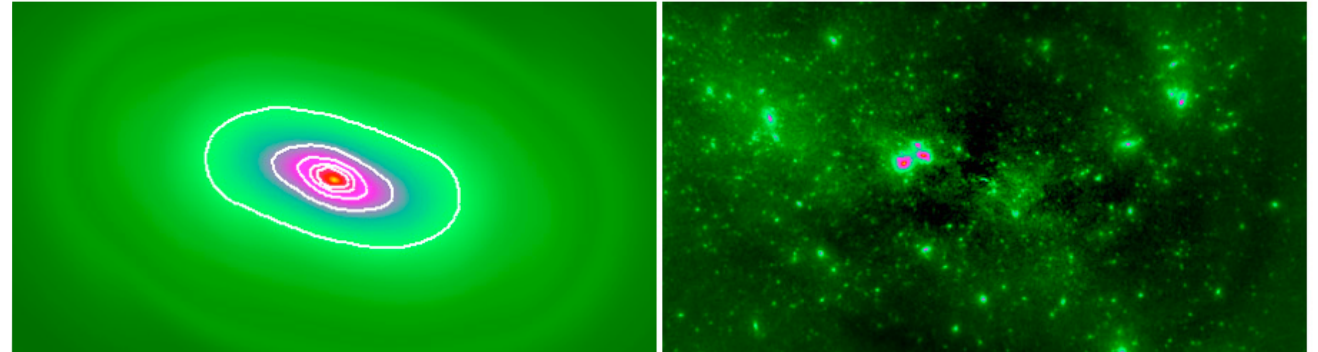


$$\kappa(\vec{x}) = \kappa_0(x) + \sum_{m=1}^{\infty} \kappa_m(x) \exp(im\phi)$$

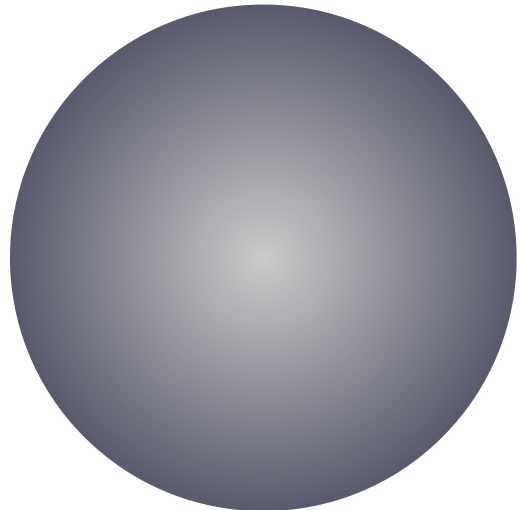
[q]

[m]

density prof. *shape*



SMOOTH COMPONENT (AND MOST IMPORTANT SUBSTRUCTURES)

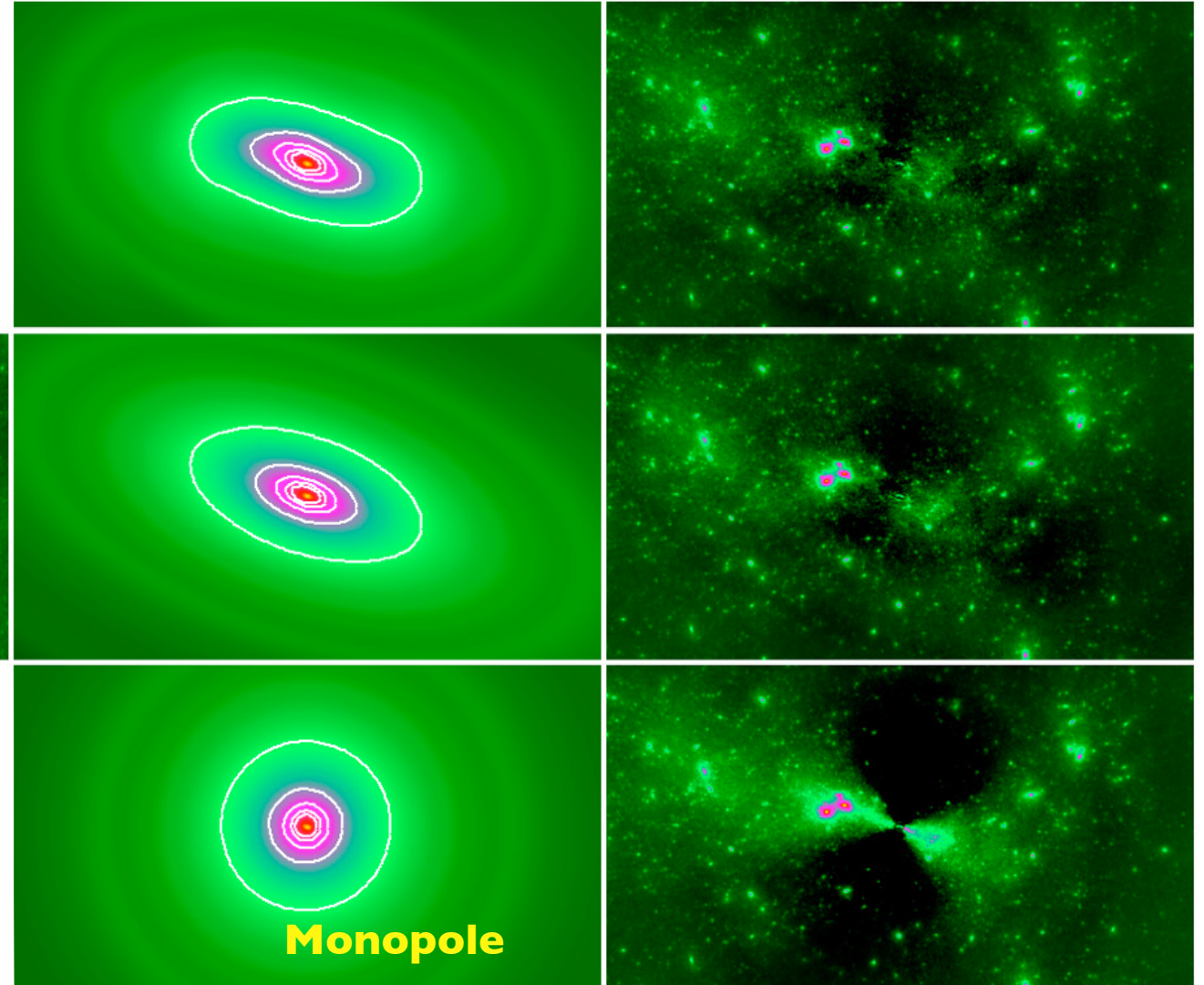


$$\kappa(\vec{x}) = \kappa_0(x) + \sum_{m=1}^{\infty} \kappa_m(x) \exp(im\phi)$$

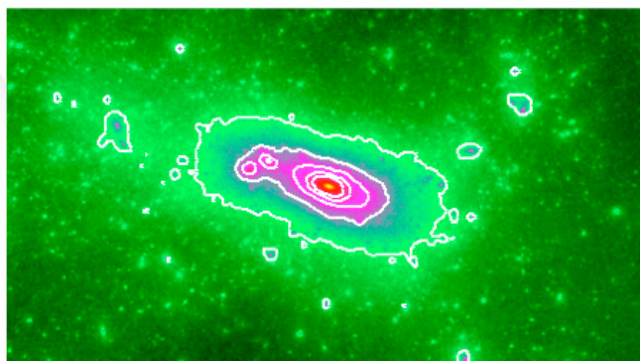
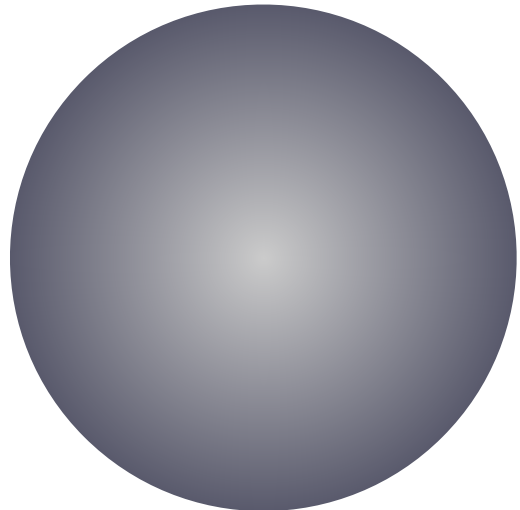
[q]

[m]

density prof. *shape*



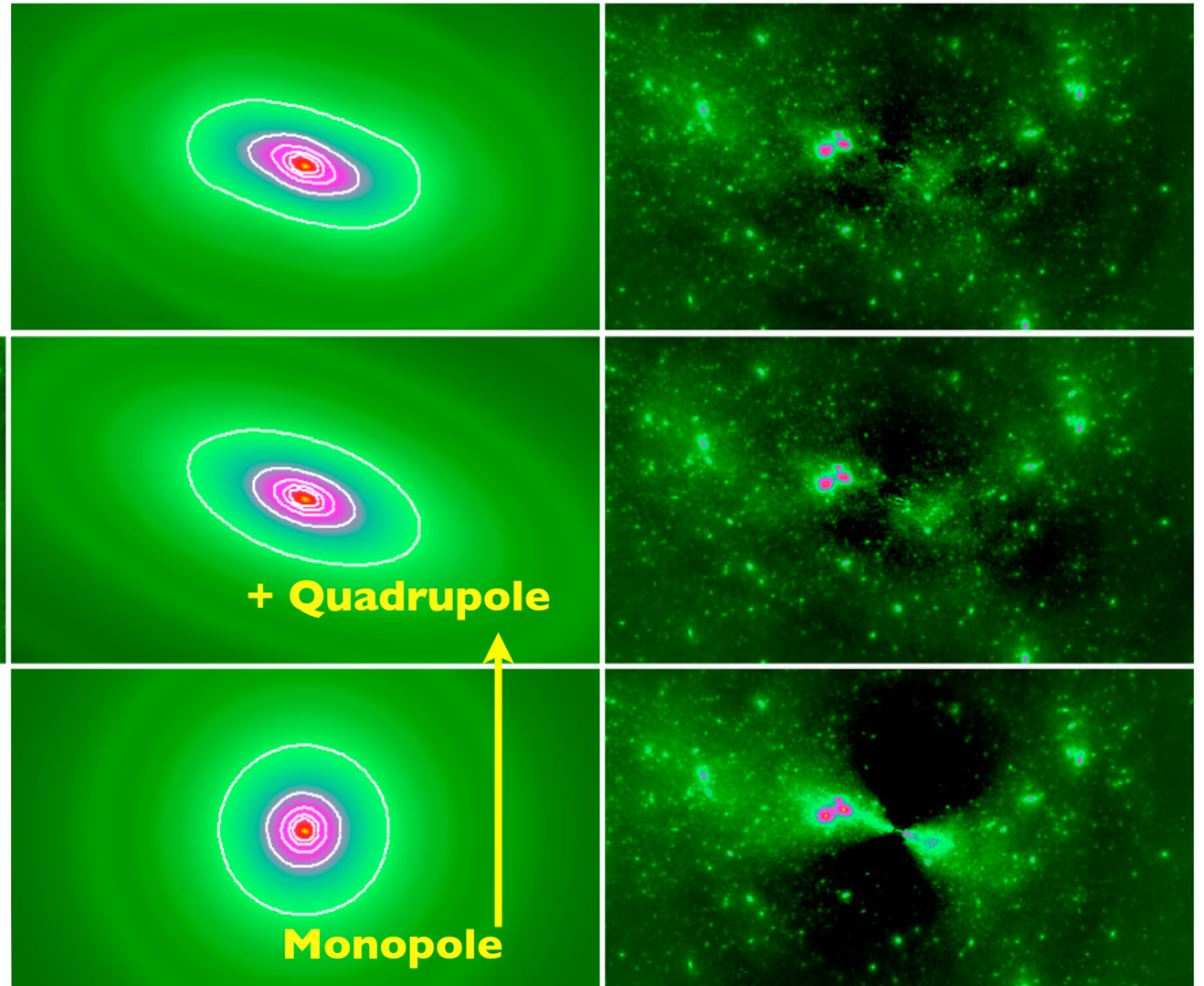
SMOOTH COMPONENT (AND MOST IMPORTANT SUBSTRUCTURES)



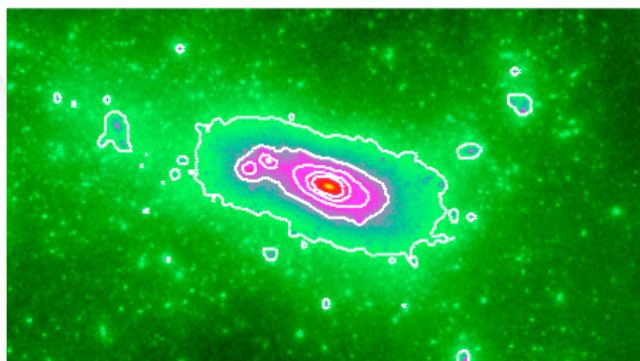
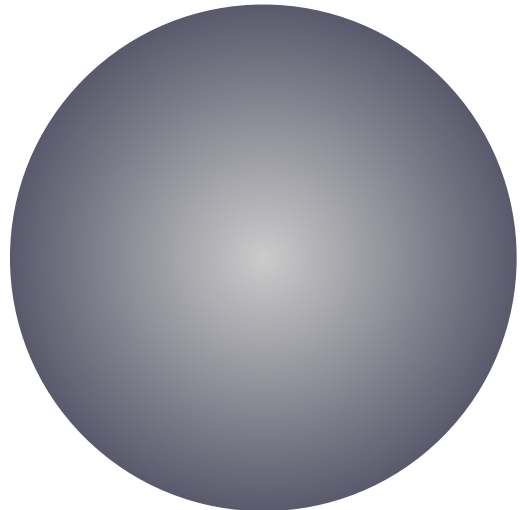
$$\kappa(\vec{x}) = \kappa_0(x) + \sum_{m=1}^{\infty} \kappa_m(x) \exp(im\phi)$$

[q] [m]

density prof. *shape*



SMOOTH COMPONENT (AND MOST IMPORTANT SUBSTRUCTURES)

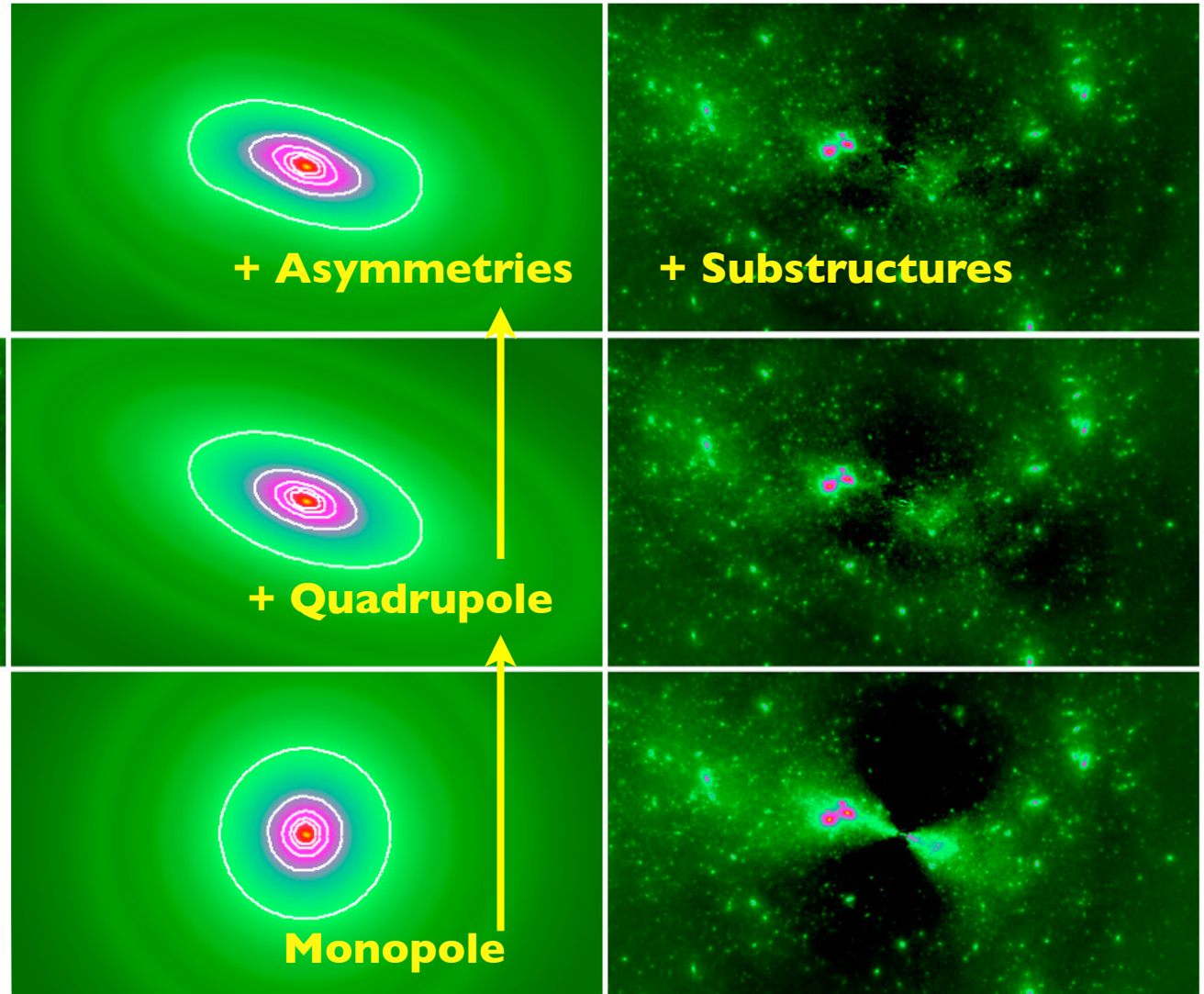


$$\kappa(\vec{x}) = \kappa_0(x) + \sum_{m=1}^{\infty} \kappa_m(x) \exp(im\phi)$$

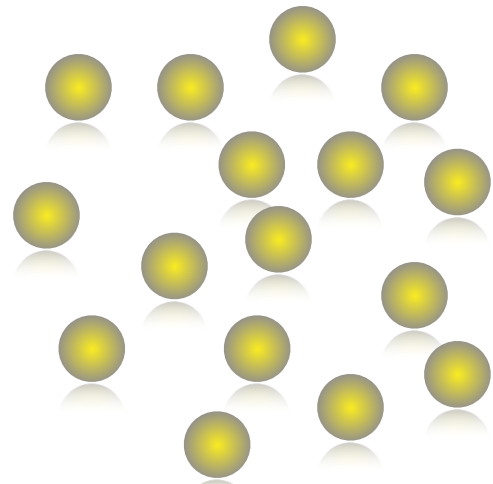
[**q**]

[**m**]

density prof. *shape*



SUBSTRUCTURES



Alternative:

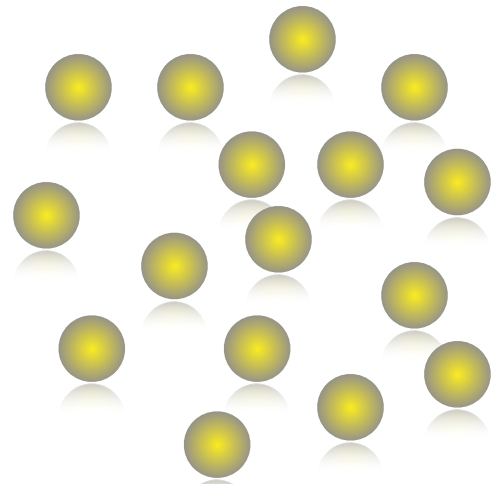
- 1) *adopt a density profile*
- 2) *fix the shape,
orientation, position*
- 3) *scale the mass using
scaling relations!*

*Impossible to optimize
each substructure
individually... (too many
parameters)*

$$\sigma = \sigma_\star \left(\frac{L}{L_\star} \right)^{1/4}$$

$$r_t = r_{t,\star} \left(\frac{L}{L_\star} \right)^\eta$$

SUBSTRUCTURES



Alternative:

- 1) *adopt a density profile*
- 2) *fix the shape,
orientation, position*
- 3) *scale the mass using
scaling relations!*

*Impossible to optimize
each substructure
individually... (too many
parameters)*

$$\sigma = \sigma_* \left(\frac{L}{L_*} \right)^{1/4}$$
$$r_t = r_{t,*} \left(\frac{L}{L_*} \right)^\eta$$

[**S**]

THE MODEL

$$\mathbf{p} = [\mathbf{q}, \mathbf{m}, \mathbf{s}, \mathbf{x}_c]$$